Università degli Studi di Padova

Dipartimento di Fisica e Astronomia

Corso di Laurea Magistrale in Fisica

Elaborato di Laurea

THE INTEGRATED SACHS WOLFE EFFECT AND ITS CROSS-CORRELATION WITH THE LARGE SCALE STRUCTURE DISTRIBUTION OF GALAXIES:
EXPLORING HIGHER-ORDER CORRELATIONS

Relatore: Bartolo Nicola

Controrelatore: Paradisi Paride

Laureando: Lionetto Luca

ANNO ACCADEMICO 2015/2016

Alla mia famiglia

Riassunto in italiano

Le anisotropie della radiazione cosmica di fondo (Cosmic Microwave Background o CMB) vengono convenzionalmente trattate al primo ordine sotto l'ipotesi di completa Gaussianità, il che le rende totalmente descrivibili dal loro spettro di potenza. Tuttavia questa potrebbe non essere una descrizione completa.

Iniziamo la tesi con una breve introduzione alla radiazione cosmica di fondo, alle sue anisotropie, e alla loro descrizione in termini dello spettro di potenza, elencando alcuni dei risultati più rilevanti ottenuti dal loro studio.

Successivamente discutiamo la possibilità dell'esistenza di non-Gaussianità della CMB abbastanza rilevanti da essere misurabili, quali informazioni fisiche potrebbero essere ricavate dalla loro analisi. Ci concentriamo in particolare sull'effetto Integrated Sachs-Wolfe (ISW), che rappresenta il contributo dominante alle anisotropie della CMB su grandi scale, e sulla non-Gaussianità generata dalla sua componente non lineare, l'effetto Rees-Sciama (RS), fornendo una sintetica descrizione di entrambi gli effetti.

Dato che l'effetto ISW è stato recentemente rilevato principalmente grazie alla sua cross-correlazione con la distribuzione della struttura su larga scala (Large Scale Structure, or LSS), forniamo una breve panoramica dello stato corrente dei cataloghi di galassie e della mappatura della LSS. Discutiamo del legame che sia l'effetto ISW che la LSS hanno con la distribuzione della massa nell'Universo, legame all'origine della loro cross-correlazione, prima di considerare la possibilità di rilevare la "firma" non-Gaussiana dell'effetto Rees-Sciama tramite un'analisi completamente relativistica, fino al secondo ordine nelle perturbazioni cosmologiche, del bispettro incrociato tra effetto ISW e sovradensità di galassie su scale ultra-larghe.

Infine, dopo un'esame dei risultati raggiunti a livello teorico nel campo di descrizioni completamente relativistiche dell' effetto ISW e della LSS fino al secondo ordine, in cui in particolare rideriviamo l'espressione per l'effetto ISW su grandi scale, forniamo le espressioni per i loro bispettri misti nelle nostre conclusioni.

Contents

1 Introduction **4**

2 The Cosmic Microwave Background **6**

2.1 CMB Power Spectrum . . . 7

2.2 Non-Gaussianity and the Bispectrum . . . 10

2.2.1 Primordial non-Gaussianities: Bispectrum shapes and inflation . . . 11

2.2.2 The CMB transfer function . . . 14

2.2.3 Secondary non-Gaussianities: Integrated Sachs-Wolfe effect . . . 15

3 Galaxy counts **16**

3.1 Surveys . . . 16

3.2 Galaxy distribution and power spectrum . . . 18

3.2.1 Galaxy Bias . . . 20

3.2.2 Evolution and Magnification Bias . . . 20

3.3 Galaxy bispectrum and nonlinear structure formation . . . 21

3.4 The growth function . . . 21

4 CMB-Galaxy Cross-Correlation **23**

5 Relativistic effects **25**

6 The Second-order CMB Radiation Transfer Function **26**

6.1 Evolution of the gravitational potentials . . . 26

6.1.1 Second-order scalar perturbations . . . 27

6.1.2 Initial conditions and primordial non-Gaussianity . . . 33

6.2 Second order ISW effect . . . 34

6.2.1 Late ISW . . . 36

6.2.2 Early ISW . . . 42

7 Relativistic corrections for galaxy counts **49**

7.1 First order corrections for redshift dependent galaxy counts 49

7.2 Projected galaxy counts and Newtonian approximation 50

8 The mixed Galaxy-ISW bispectrum **50**

8.1 Multipole terms - ISW 51

8.2 Multipole terms - Galaxy Counts 53

8.2.1 Projected galaxy counts 53

8.2.2 Redshift-dependent relativistic galaxy counts at first order 54

8.3 Redshift-dependent bispectrum terms 54

8.4 ISW-Projected galaxy counts bispectra 56

9 Summary and Conclusions **58**

A N-point correlation functions **60**

A.1 2-point correlation function and power spectrum 60

A.2 3-point correlation function and bispectrum 61

B Wigner 3-j Symbols **62**

B.1 Definition 62

B.2 Properties 62

B.3 The Gaunt Integral 63

Abstract

Anisotropies of the Cosmic Microwave Background (CMB) are conventionally treated linearly under the hypothesis of complete Gaussianity, which allows them to be fully described by their power spectrum. However, this may not be a complete description. We give a brief introduction to CMB anisotropies, highlighting the role of their study in modern cosmology, before considering whether measurable CMB non-Gaussianities exist, their statistical description in terms of the bispectrum (i.e. the Fourier counterpart of the 3-point correlation function), and what physical information could be gained by their analysis. We focus in particular on the integrated Sachs-Wolfe (ISW) effect, the dominant CMB anisotropy contribution on large scales, and the non-Gaussianity generated by its nonlinear component, the Rees-Sciama effect. As the ISW effect was recently detected through its cross-correlation with the distribution of the Large Scale Structure (LSS), we give a brief overview of the current status of galaxy surveys and LSS mapping, before considering the possibility of detecting the non-Gaussian signature of the Rees-Sciama effect by means of a fully relativistic analysis, up to second order in the cosmological perturbations, of the cross ISW-Galaxy overdensity bispectra on ultra-large scales. Finally, after an examination of the theoretical achievements in the field of second-order, fully relativistic description of both CMB and LSS anisotropies, we write down the expressions for such bispectra in our conclusions.

1 Introduction

One of the cornerstones of the Cosmological Standard Model is the theory of *cosmological inflation* - which posits that the early Universe underwent a phase of extremely rapid expansion, dramatically increasing in size (enough for quantum-scale fluctuations to be redshifted out of the horizon). This theory answers several questions concerning the existing observational data, such as the measured curvature of the universe (flatness problem), the apparent homogeneity among parts of the Universe which should not otherwise have been in causal contact (horizon problem) and the lack of observable topological defects like cosmic strings and monopoles. At the same time, cosmic inflation provides an explanation for both the relative homogeneity of the cosmic microwave background and its initial anisotropies, which in turn are necessary to explain structure formation. Because of their importance, Cosmic Microwave Background (CMB) anisotropies and their distribution have been the subject of intensive research, first of all focused on their two-point correlation function and its Fourier transform, the power spectrum, which has resulted in a wealth of information about the Universe's composition and structure.

However, the knowledge provided from the CMB power spectrum, and from the complimentary study of the Large Scale Structure (LSS) two-point distribution function, is still far from complete, especially concerning the nature of cosmological inflation itself: while our information about the amplitude and scale-dependence of primordial fluctuations is enough to rule out several classes of cosmological models, there are still many possible inflationary models which are virtually undistinguishable in terms of their primordial power spectrum. The reason for this is that the power spectrum is determined just by the (potentially time-dependent) inflationary expansion rate and therefore by the inflationary energy density, but does not constrain the interaction of the field (or fields) associated with it.

Stopping at the two-point correlation function, however, is only acceptable if it represents *all* the available information about the statistical distribution of the cosmological perturbations, which would happen only if such statistical distribution was completely Gaussian. In the event of any deviation from a perfectly Gaussian distribution, that is, any non-Gaussianity, higher order correlators which are no longer expressed in terms of the two-point function and, in particular, uneven higher order correlators such as the three-point function are no longer identically zero. In such a case, therefore, their study can yield information which is not encoded in the power spectrum.

While non-Gaussianity has been the subject of research for almost thirty years, (mainly in studies concerning the distribution of the Large Scale Structure), until the end of the last decade most of the attention was focused on the two point correlations. There are several reasons for this:

- Higher order correlation functions (or power polyspectra) are analytically complex and computationally intensive to calculate.
- Given the strongly Gaussian character and small relative amplitude of CMB anisotropies ($\sim 10^{-5}$), it was thought any non-Gaussianity would be too small to be measurable.
- The standard, single field, slow-roll model of inflation is expected to produce small and likely unobservable non-Gaussianity.
- Even the data collected from the Planck satellite so far, while enough to place the most stringent limits on non-Gaussianity up to now, has yet to conclusively detect such a signal.

While the Large Scale Structure shows high non-Gaussianity in its distribution, most of it is due to the action of gravitational instability, an intrinsically nonlinear phenomenon, and is therefore present even in the case of Gaussian initial conditions. Our ability to constrain or detect primordial non-Gaussianity in this way is therefore limited by our ability to distinguish it from that due to gravitational evolution, a task made more difficult by the relation between primordial non-Gaussianity and the galaxy bias itself, that is, the relation between matter and galaxy distributions. However, because of the uncorrelated sources of noise in the CMB anisotropy and Galaxy distributions, cross-correlating them has been proved to significantly increase the signal-to-noise ratio of, for example, the Integrated Sachs-Wolfe (ISW) effect. It is therefore possible that cross-correlation of Planck data with that available from a future, Euclid-like survey may be enough to detect non-Gaussianity at the level of second-order perturbation theory.

This work will be structured as follows:

Section 2 will consist in an introduction to the Cosmic Microwave Background, its power spectrum and the current cosmological results, followed by an explanation of CMB non-Gaussianity. We will also describe CMB anisotropies sensitive to it, such as the Integrated Sachs-Wolfe (ISW) and Rees-Sciama effects and detail the correlation between non-Gaussianity and inflationary models, with an emphasis on the link between inflationary conditions and bispectrum shapes.

In Section 3, will consist in a brief study of non-linear gravitational instability and structure formation, and of its links with the galaxy bispectrum.

In Section 4 we will introduce the topic of CMB-Galaxy count cross-correlation and explain its usefulness in ISW measurements

In Section 5 we will consider relativistic corrections to both CMB and galaxy bispectra and discuss why they may be relevant

In Section 6 we will retrace the steps of article [24] to re-obtain the second order transfer function for large-scale CMB anisotropies.

In Section 7, we discuss the impact of general relativistic corrections on galaxy counts.

In Section 8, which will be the core of this work, we will use the CMB transfer function thus found to discuss the mixed ISW-galaxy bispectrum at large scales.

Finally, Section 9 will consist in a brief summary and discussion of our conclusions.

2 The Cosmic Microwave Background

The Cosmic Microwave Background, first discovered in 1964 by Penzias and Wilson (Nobel Prize 1978), is, as the name suggests, an almost uniform and isotropic radiation background which permeates the Universe. It is, as the COBE mission famously demonstrated, an almost perfect example of blackbody radiation, with a temperature of 2.725 K. It is sometimes called a “fossil” radiation, in that its constituent photons were generated at the recombination epoch, (about 379,000 years after the Big Bang) and had almost no interaction with the surrounding Universe since then. This makes it the oldest image of the Universe we have access to (outside of neutrino and gravitational astronomy), and therefore the greatest available source of data on the conditions of the early Universe, (together with the data on primordial nucleosynthesis). In fact, its very existence (and blackbody spectrum) is one of the main observational underpinnings of Big Bang cosmology and the Standard model of cosmology, in that it proves the Universe began in (or at least went trough) a high-density, high temperature state from which it later expanded and cooled.

Despite the great significance of the CMB's almost perfect isotropy, it is its *anisotropies* (first detected by the COBE-DMR experiment in 1990 [98]) which hold a great deal more information about the primordial Universe. If the primordial plasma had been perfectly uniform, in fact, no structure formation through gravitational instability could have taken place [39, 81], so at least some *primordial* anisotropy must have existed, and since the CMB photons were once in thermal equilibrium with the primeval plasma, their temperature (and polarization) fluctuations should reflect these perturbations.

Additionally, according to the Cosmological Standard Model, primordial anisotropies are due to small, quantum-scale fluctuations in the inflaton field, which were stretched to cosmic scales by the very inflationary process and formed the seeds for the subsequent structure formation, making the study of CMB anisotropies a potential source of information on the physics behind cosmic inflation [20, 57, 68, 100].

Finally, *secondary* microwave background anisotropies, those deriving from the gravitational interaction of the CMB photons with the rest of the Universe, from the recombination epoch onwards are a potential source of information on structure formation, gravity and the presence and nature of both dark matter and dark energy.

Due to their link to both the nature of the primordial Universe and its current structure, CMB anisotropies have been subject of intense study. In less than 25 years, three major space missions (COBE (1989), WMAP (2003)[14] and Planck (2012)[7]) have been launched with the stated goal of measuring the cosmic microwave background temperature and polarization anisotropies with increasing sensitivity and precision, an effort complemented by scores of ground- and balloon-based experiments (Such as [3], [41], [66], [84], and [85]), yielding an impressive amount of data (see [8], and [14] for two of the most comprehensive reviews on the subject).

Due to the small ($\sim 10^{-5}$) magnitude of CMB anisotropies, both their creation and following evolution have traditionally been treated in the linear regime. In this approximation, the initial fluctuations are completely Gaussian: they are uncorrelated and have random phases, which means they can be efficiently described by means of their two-point correlation function and its Fourier transform, the power spectrum.

2.1 CMB Power Spectrum

Since the distribution of the anisotropies is isotropic, it is possible to study their power spectrum in Fourier space (see Appendix A), but since the measured CMB temperature depends on a specific direction in the sky, and the sky itself is not flat, rather than use a Fourier transform it is more appropriate to expand the temperature anisotropies of the CMB

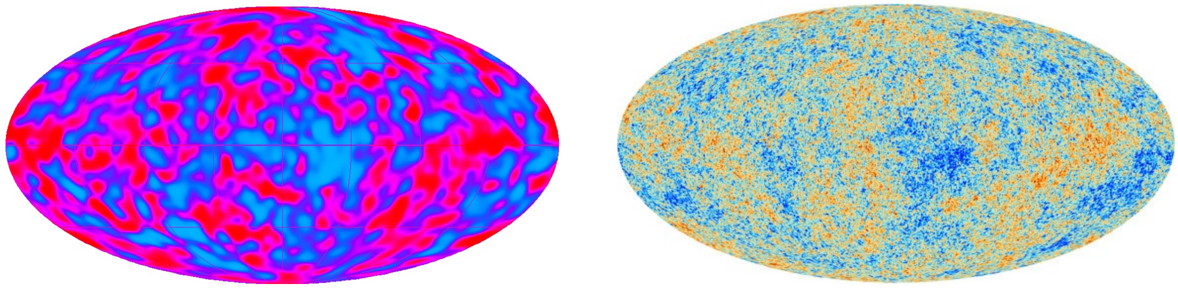

Figure 1: The CMB sky anisotropies as measured by COBE (left) and Planck (right). Increased sensitivity and angular resolution in available background measurements have started what has been called "the era of precision cosmology". (source: COBE collaboration, Planck Collaboration)

in spherical harmonics

$$\frac{\Delta T(\hat{n})}{T} = \sum_{lm} a_{lm} Y_{lm}(\hat{n}), \tag{1}$$

and define the power spectrum in terms of the joint average of the harmonic coefficients a_{lm}

$$P^{l_1 l_2}_{m_1 m_2} = \langle a_{l_1 m_1} a_{l_2 m_2} \rangle \,. \tag{2}$$

Because of its rotational invariance, however, the CMB power spectrum is also often defined in terms of the coefficients C_l defined by

$$\langle a_{lm} a^*_{l'm'} \rangle = C_l \delta_{ll'} \delta_{mm'}. \tag{3}$$

As previously mentioned, for Gaussian field fluctuations all higher order correlators are either functions of the power spectrum (as is the case of even-numbered functions) or identically zero (in the case of odd-numbered ones). Therefore, under the Gaussian hypothesis, the power spectrum contains *all* the statistical information of the CMB anisotropy map.

The wealth of information gained from the study of the CMB power spectrum has been staggering: it has been said to have turned Cosmology from a data starved into a data driven science. The Cosmological Standard Model of the Universe, which is largely based on it, describes a 13.8 billion year old, spatially flat (within 1%) Universe, composed for 68.5% by a Dark Energy (DE) component or a cosmological constant Λ, for 26.6% by a Dark Matter (DM) component, and for 4.9% by ordinary matter, and does so with only a few parameters: the amplitude and scale dependence of primordial fluctuations, the baryon, DM and DE energy densities and lastly the optical depth due to hydrogen reionization [8, 14].

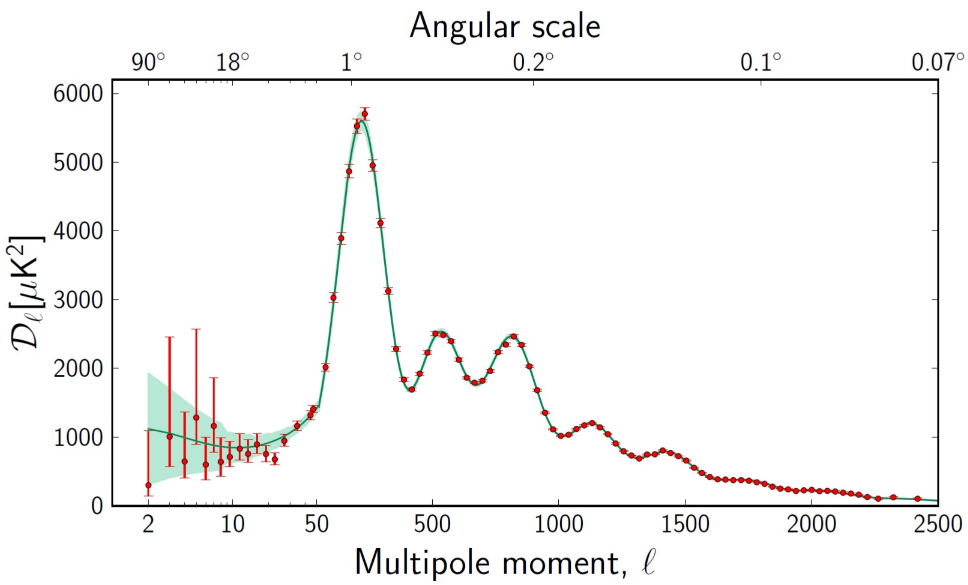

Figure 2: Angular power spectrum of CMB temperature fluctuations from *Planck*. The error bars include cosmic variance, which is also shown as the shaded area around the best-fit curve. (source: Planck collaboration)

The Cosmological Standard model, while able to *describe* the Universe, does not fare as well when it comes to *explaining* it. It postulates the existence of two dark components making up about 95% of the universe, but provides little information about their nature. It posits the existence of an initial phase of accelerated expansion in the form of Inflation, and provides tight constraints on the physical processes running it and on its role in the generation of primordial anisotropies, but the specific model has not been precisely pinned down (the primordial perturbations might be for example be due to a different field from the inflaton, such as in the curvaton model [21]).

This is due, at least in part, to the nature of the two point function. As already mentioned, in the Gaussian hypothesis fluctuations are *uncorrelated*, which means they are by necessity non-interacting. Tracing back from CMB fluctuations to the field that generated it, this means that the power spectrum is unable to describe the interactions of the inflationary field. This is not surprising: in quantum field theory, two-point correlation functions of fields describe free particles propagating in spacetime, while each interaction requires vertices, and therefore higher order correlators. Even in the case of secondary anisotropies, a linear approach cannot fully take into account markedly non-linear phenomena like, for example, gravitational instability and the evolution of cosmic structures, or the second-order CMB anisotropies unavoidably generated by gravity, which is non linear.

While the linear approximation has been an excellent one, it has perhaps begun to show its limits. The natural response is to start considering non-linear terms, which in turn involves dropping the assumption of complete Gaussianity. The question therefore becomes whether *measurable* CMB non-Gaussianities exist and what physical information can potentially be gained from their study.

2.2 Non-Gaussianity and the Bispectrum

The study of the possible non-Gaussianity of the Cosmic Microwave Background has been ongoing since the eighties, but it has only recently risen to the forefront of cosmological research. This is due to a combination of factors, among which the possibility, thanks to the data from missions like WMAP and Planck, to either detect primordial non-Gaussianity or provide meaningful physical constraints. Given the difficulty in measuring higher-order correlation functions due to noise and cosmic variance, most of the ongoing studies focus on the lowest non-Gaussian indicator, the bispectrum $B_\phi(k_1, k_2, k_3)$ defined as

$$\langle \phi(\mathbf{k}_1)\phi(\mathbf{k}_2)\phi(\mathbf{k}_3)\rangle = (2\pi)^3 \delta_D\left(\mathbf{k}_1 + \mathbf{k}_2 + \mathbf{k}_3\right) B_\phi(k_1, k_2, k_3). \tag{4}$$

As the bispectrun is an odd-numbered correlation function, its detection would automatically rule out the hypothesis of a completely Gaussian anisotropy distribution. In terms of spherical harmonics the bispectrum is given by [99]

$$B^{l_1 l_2 l_3}_{m_1 m_2 m_3} = \langle a_{l_1 m_1} a_{l_2 m_2} a_{l_3 m_3} \rangle \, . \tag{5}$$

As in the power spectrum case, if we assume rotational invariance it is possible to factorize the m-dependence out of this expression, and work with the *reduced* bispectrum $b_{l_1 l_2 l_3}$ defined by

$$B^{l_1 l_2 l_3}_{m_1 m_2 m_3} = \mathcal{G}^{l_1 l_2 l_3}_{m_1 m_2 m_3} b_{l_1 l_2 l_3}, \tag{6}$$

where $\mathcal{G}^{l_1 l_2 l_3}_{m_1 m_2 m_3}$is the Gaunt integral, which we describe in more detail in Appendix B.

As mentioned in the introduction, the three-point function, when different from zero, encodes information not present in the power spectrum, because it is sensitive to *non linear* phenomena, such as interactions between inflationary fields, the non-linear evolution of the photon-baryon fluid and second-order general relativistic effects. These effects can either belong to the pre-recombination epoch, in which case they influence the primary CMB anisotropies, including primordial non-Gaussianity from inflation, or they can be tied to photon interactions after recombination, in which case they influence secondary CMB anisotropies. In the following sections, we will explore how, in both cases, their study can yield useful physical constraints on the processes involved in their formation.

2.2.1 Primordial non-Gaussianities: Bispectrum shapes and inflation

As we can see in Appendix A, the delta function present in the expression for the bispectrum in Fourier space constrains the magnitude of the three wavevectors, whose sum must equal zero. Even the angular bispectrum satisfies the triangular condition $|l_i - l_j| \leq l_k \leq l_i + l_j$ and $m_1 + m_2 + m_3 = 0$. We note two properties of this triangle condition: the first is that, since a triangle can be completely described by the length of its three sides, then in the isotropic case we can describe the bispectrum only in terms of the wavenumbers k_1,k_2,k_3 (or of the multipole indices l_1,l_2,l_3). The second is that the presence of three parameters in the delta function allows for a greater range of combinations than the two-parameter case, where the two vectors are constrained to have the same magnitude.

The very shape of the bispectrum can therefore potentially give us a wealth of cosmological information. In fact, the biggest step in this sense has been made in the nineties, with the discovery of an important relation between non-Gaussianity and the possible physical mechanics behind inflation. It was found that the only models of inflation which do not produce detectable non-Gaussianity are those who respect *all* of the following conditions [21]:

1. There is only a single field driving inflation, and its fluctuations generated the initial perturbations that were the seeds for structure generation

2. The kinetic term of the quantum field is canonical, resulting in a fluctuation propagation speed equal to the speed of light
3. The 'slow roll' condition, stating that the evolution of the field is always very slow compared to the Hubble time during inflation, is satisfied
4. The quantum field was in a Bunch-Davies vacuum state before the quantum fluctuations were generated during inflation

Moreover, it was found that the violation of any one of this four conditions would not only produce a detectable amount of non-Gaussianity, but that the associated bispectrum would have a *specific shape* associated with it. For example multi-field models would generate CMB anisotropies with a signal that peaks for squeezed triangles, models with non-canonical kinetic terms would give rise to a bispectrum peaking for equilateral triangles, non adiabatic vacuum models would result in a folded triangle bispectrum configuration, etc, while multiple violations of the above conditions would result in a combination of different shapes [37, 38]. The shape of the bispectrum is therefore a powerful instrument to discriminate between inflationary models who would otherwise lead to very similar power spectra [11].

Because of their significance, there is an ongoing effort to detect such bispectrum shapes in the CMB signal. This is mainly done by introducing a non-linearity parameter f_{NL} describing the amplitude of eventual non-Gaussianities. In the squeezed bispectrum case, for example, f_{NL} is defined by [65]

$$\phi(\mathbf{x}) = \phi_g(\mathbf{x}) + f_{NL}\phi_g^2(\mathbf{x}), \tag{7}$$

with $\phi(\mathbf{x})$ the primordial gravitational potential from inflation, with $\phi_g(\mathbf{x})$ a Gaussian field. Analysis of current data from Planck did not detect a signal, but was able to constrain the value of f_{NL} for the most studied shapes [11]: $f_{NL}^{equilateral} = -16 \pm 70$, $f_{NL}^{squeezed} = 2.5 \pm 5.7$, $f_{NL}^{orthogonal} = -34 \pm 33$.

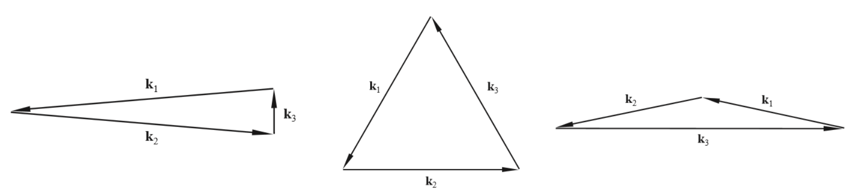

Figure 3: Three possible bispectrum shapes. The left one represents a squeezed bispectrum for $k_1 \ll k_2 \sim k_3$, the middle one, with $k_1 = k_2 = k_3$ represents the equilateral bispectrum and the right one represents a folded bispectrum for $k_1 \sim k_2 + k_3$ (source: [67])

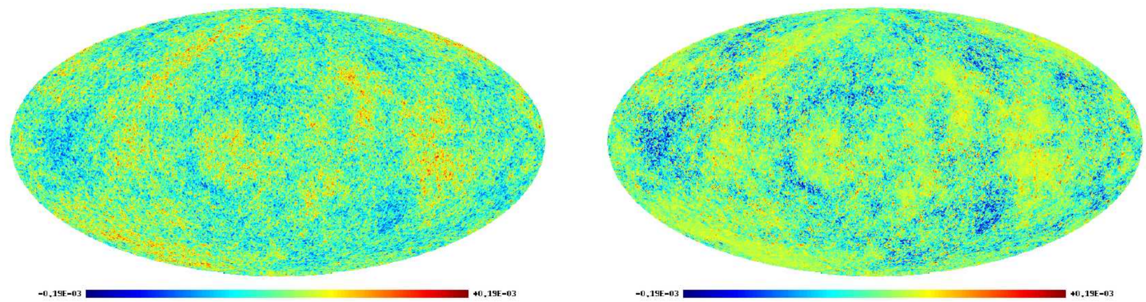

Figure 4: Two simulations of the CMB sky. The left one is completely Gaussian, while the right one has been obtained from the first by adding a non-Gaussian component with $f_{NL} \sim 3000$. Measurements from the Planck mission constrain the value of f_{NL} to the order of unity. (source: Liguori, M., Matarrese, S., & Moscardini, L. 2003, Astrophys. J. , 597, 57)

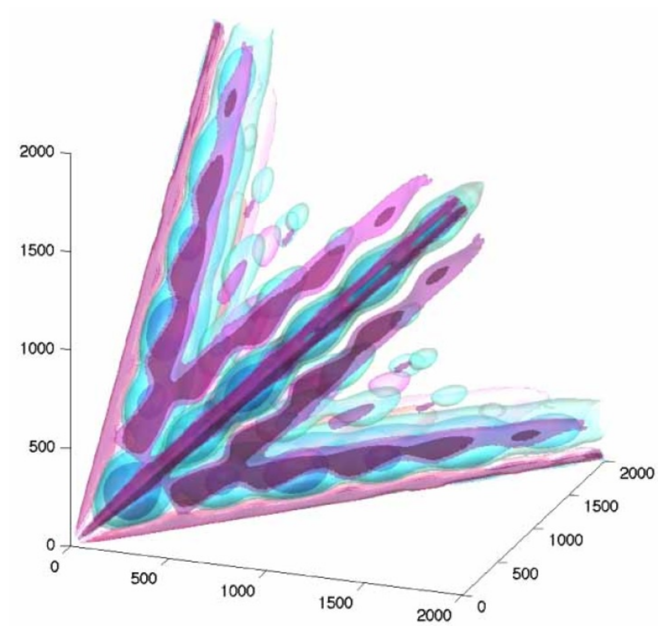

Figure 5: Example of (reduced) bispectrum where non-Gaussianity is largely generated by local mechanisms. Each axis indicates the value of a multipole l, with the amplitude of the respective signal color coded from blue (low), to purple (high). As can be seen, the signal is dominated by the squeezed shape. (source: Fergusson, J. R., & Shellard, E. P. S. 2009, Phys. Rev. D , 80, 043510)

2.2.2 The CMB transfer function

When considering primordial fluctuations of the inflationary field, it is important to keep in mind that these are not the same as those *observed* in the CMB. Rather, the observed anisotropies represent the combination of those *primary*, intrinsic anisotropies and a number of *secondary* ones, due to the photon traveling along the path from the last scattering surface to the observer. In Fourier space, this is represented by the convolution of the original anisotropy function with a *transfer function* describing evolution of the primordial perturbations.

At first order, the relation between the multipoles of the primordial potential ϕ and the CMB ones is determined by a convolution with the transfer function $\Delta_l^{(1)}(k)$, which describes the linear perturbation evolution (the so-called CMB radiation transfer function) [73]

$$a_{lm} = 4\pi(-i)^l \int \frac{d^3k}{(2\pi)^3} \phi_{1i}(k) \Delta_l^{(1)}(k) Y_{lm}^*(\hat{k}). \tag{8}$$

By replacing (8) in (2) and (5) we get

$$P^{l_1 l_2}_{m_1 m_2} = (4\pi)^2 (-i)^{l_1+l_2} \int \frac{d^3k_1}{(2\pi)^3} \frac{d^3k_2}{(2\pi)^3} \Delta(k_1) \Delta_{l_2}(k_2) \langle \Phi(\mathbf{k}_1) \Phi(\mathbf{k}_2) \rangle , \tag{9}$$

which in the case of rotational invariance reduces to

$$C_l = (4\pi)^2 (-i)^{l_1+l_2} \int \frac{d^3k_1}{(2\pi)^3} \Delta_{l_1}^2(k) \langle \Phi^*(\mathbf{k}) \Phi(\mathbf{k}) \rangle , \tag{10}$$

for the CMB power spectrum, and

$$B^{l_1 l_2 l_3}_{m_1 m_2 m_3} = (4\pi)^3 (-i)^{l_1+l_2+l_3} \int \frac{d^3k_1}{(2\pi)^3} \frac{d^3k_2}{(2\pi)^3} \frac{d^3k_3}{(2\pi)^3} \Delta(k_1) \Delta_{l_2}(k_2) \Delta_{l_3}(k_3) \times$$

$$\langle \Phi(\mathbf{k}_1) \Phi(\mathbf{k}_2) \Phi(\mathbf{k}_3) \rangle Y_{l_1 m_1}(\hat{\mathbf{k}_1}) Y_{l_2 m_2}(\hat{\mathbf{k}_2}) Y_{l_3 m_3}(\hat{\mathbf{k}_3}), \tag{11}$$

for the CMB bispectrum.

Of course while such a transfer function may (implicitly) account for the presence of non-Gaussianities in the *initial* fluctuations, it still assumes their evolution to be linear, and thus secondary anisotropies to be completely Gaussian. On the other hand, as we will see, a second-order estimation of secondary anisotropies not only helps further constrain and disentangle the primordial non-Gaussian signal, but is a source of physical information in its own right.

2.2.3 Secondary non-Gaussianities: Integrated Sachs-Wolfe effect

The Integrated Sachs-Wolfe (ISW, for short) effect is one of the secondary anisotropies of the cosmic background radiation, caused by the variation in time of the gravitational potential (or, in relativistic terms, of the metric) along the line of sight [88]. In fact, unless the evolution of density perturbations matches the expansion rate of the Universe, the gravitational potential ϕ will evolve in time, causing in turn a net frequency variation in the photons crossing it. In intuitive (though not exact) terms, if the gravitational potential in a region changes with time, the "slope" a photon happens to "fall into", may be higher or lower than the potential well it has to "climb out of", with the net result being an increase (or decrease) in photon energy. the resulting line-of-sight fractional fluctuation in observed CMB temperature is given by

$$\frac{\Delta T}{T}(\hat{n}) = \int_{\eta_L}^{\eta_0} d\eta \phi'(\mathbf{x}, \eta) \Big|_{\mathbf{x}=-\hat{\mathbf{n}}(\eta_0-\eta_L)}, \tag{12}$$

where η is the cosmic time, with η_0 the present epoch and η_L the time corresponding to hydrogen recombination (and therefore the last scattering surface). Study of this phenomenon has been performed using both Newtonian and fully relativistic formalism, by expanding the perturbations in the gravitational potential to first or second order. As we will see, the first and second order terms have remarkably different behaviors.

The linear contribution is called "linear ISW" (or often just ISW) effect, and vanishes in matter-dominated, spatially flat Universes due to the constancy, *at first order*, of the gravitational potential in time. However, if the equation of state of the Universe *varies*, in general this causes a gradual decay of the gravitational potentials, which can give a strong contribution on large scales. According to the Cosmological Standard Model, this has happened two times, first with the transition from the radiation, dominated to the matter-dominated epoch, and finally in (relatively) recent times, with the transition from a matter-dominated epoch to a cosmological constant/dark energy dominated epoch. These two transitions give rise to the Early ISW and Late ISW respectively.

The second-order contribution, or Rees-Sciama (RS) effect [86] is due to the nonlinear collapse of initial perturbations and the ensuing structure formation, which can cause the gravitational potential to change in time even in a flat, matter dominated Universe, modifying the energy of CMB photons as they cross nonlinear structures. This effect dominates at small scales (large k) as such scales are where the nonlinear nature of structure formation becomes relevant.

Both ISW and Rees-Sciama effects are of great interest to cosmologists because of their dependence on both the variation of the gravitational potentials and structure growth. They provide a tool to measure the *dynamical* effect of the dark energy component on the evolution of cosmic structure, and as such are sensitive not just to the amount, but to the nature and the clustering properties of DE, contributing to break the degeneracy between different dark energy models (such as Cosmological Constant, Quintessence and many Unified Dark Matter models) [47] and between DE and possible deviations from General Relativity at large scales [17, 87].

Moreover, as we will see in Section 6, the completely relativistic expression for the ISW effect at second order presents a term dependent on *primordial* non Gaussianity, offering a new avenue of research for f_{NL} detection and measurement.

Study of first and second order integrated Sachs-Wolfe effect is not without difficulties, however, with the greatest practical challenge being the low amplitude of their signal. The linear ISW contribution to CMB anisotropies is very weak, and while it dominates for low multipoles, cosmic variance is also very high at such scales. The RS effect, on the other hand, despite being the dominant secondary anisotropy for medium-small scales $100 \lesssim l \lesssim 1000$ has been shown by numerical simulations to be negligible in comparison with primary anisotropies at those scales [103].

It is fortunate then, that the CMB is not our only tracer of primordial anisotropies and their evolution.

3 Galaxy counts

While, according to the Cosmological Principle, the Universe is homogeneous and isotropic (for a comoving observer), this is only true on very large scales. On smaller scales matter appears to have a very inhomogeneous, hierarchical distribution with galaxies, galaxy clusters and superclusters making up even larger "sheets", "walls" or "filaments" separated by vast underdense regions known as "voids", in a sponge-like arrangement known as Large-Scale Structure (LSS)[43, 109, 104]. The discovery of this "Cosmic Web" is relatively recent [43, 104] and due in large part to technical advances in the fields of optical and IR telescopes, data acquisition and digitalization (with the transition from photographic plates to CCDs) and data sorting and matching algorithms, which made the systematic analysis of vast amounts of astronomical data feasible and ushered in the age of modern sky surveys.

3.1 Surveys

The history of galaxy catalogs is almost as old as the discovery of extragalactic objects, but the first, modern galaxy redshift surveys (i.e. galaxy catalogs which use measurements of redshift, together with angular position, to create *three-dimensional* maps of the sky) started in the early 80s, with the CfA redshift survey [43], followed in the early 90s by large scale surveys like ORS [91] and IRAS [101, 78, 79] combining IR and optical catalogs.

Technical and observation time constraints usually force a trade off between sky coverage, amount of objects observed and survey depth (this problem as been ameliorated by the introduction of "photometric redshift" measurements, but true, spectroscopic redshift measurements remain preferable). For example, the beginning of the twenty-first century saw the beginning of the Two Micron All-Sky Survey (2MASS) [59], which produced an all sky catalog of the local Universe with 91% coverage, but a relatively shallow maximum redshift of $z = 0.03$, and the 2dFGRS, 6dFGS and Sloan Digital Sky Survey (SDSS) [1, 2, 12], which had more limited coverage (8%, 40% and 35% of the sky respectively) but included objects at much higher redshift (up to $z = 0.33$).

Recently, galaxy datasets covering the whole sky at a variety of redshifts have been obtained by cross-matching measurements from several different catalogs (see e.g. [30, 60]). Finally, planned surveys like that which will be provided by the Euclid satellite mission [4, 5] and by the Square Kilometer Array [34, 83] are expected to produce full coverage surveys for very high redshift values ($z \simeq 2$) which will not only provide an unprecedented amount of data on galaxy and galaxy clustering, but allow studies of their cross-correlation with large-scale CMB anisotropies.

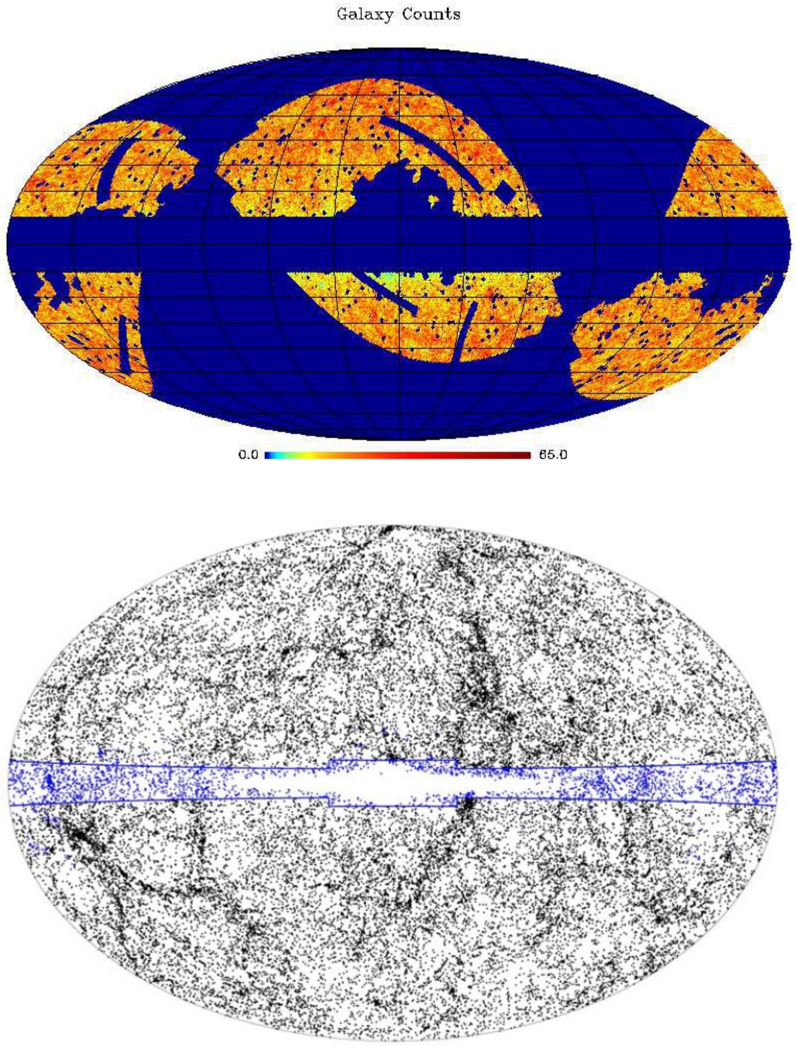

Figure 6: Above: sky coverage of the WISE galaxy survey. Below: Sky coverage for the 2MASS redshift survey. Recent surveys have dramatically increased the scales at which the Galaxy overdensity spectrum can be studied. (credit: WISE Collaboration, 2MASS Collaboration)

3.2 Galaxy distribution and power spectrum

The test of the Large Scale Structure is motivated by several reasons: first, an observation of the homogeneity and isotropy of the local Universe provides, within the relative limits, some degree of experimental backing to the Cosmological Principle. Secondly, by analyzing the cosmic web at different redshifts we can obtain valuable information on the mechanisms behind structure formation and evolution. Thirdly, as the Cosmic Web was generated by the evolution of the primordial perturbations visible in the CMB, it can be used to further test and constrain the initial conditions from inflation. Finally, it can be used to test the behavior of General Relativity on large scales.

To this end, we once again resort to the anisotropy distribution function, with the temperature field replaced by the number of observed galaxies.

We define galaxy number counts as the relative difference between the galaxy number density in a certain direction of observation (and at a certain redshift) $n_g(\mathbf{n}, z)$ and its value in an homogeneous and isotropic FRW background $\bar{n}_g(z)$

$$\delta_g(\mathbf{n}, z) = \frac{n_g(\mathbf{n}, z) - \bar{n}_g(z)}{\bar{n}_g(z)}. \tag{13}$$

Like in the case of the CMB, we can calculate the two-point correlation function of these anisotropies and their power spectrum. However, since galaxy overdensity depends on redshift, so will both functions

$$P^{l_1 l_2}_{m_1 m_2}(z_1, z_2) = \langle a_{l_1 m_1}(z_1)\, a_{l_2 m_2}(z_2)\rangle . \tag{14}$$

It is often more useful to consider the *line-of-sight projected galaxy counts*, that is, the total galaxy count anisotropy for a certain angular position, integrated over all redshifts [92]

$$\delta_g(\mathbf{n}) = \frac{n_g(\mathbf{n}) - \bar{n}_g}{\bar{n}_g} = \int_{z_s}^{z_e} dz n(z)\, \delta_g(\mathbf{n}, z), \tag{15}$$

where z_s and z_e are the minumum and maximum redshifts considered by our survey, and$n(z)\,dz$ is the redshift distribution of the considered galaxies. For the latter we use the standard parametrization [92, 96]

$$n(z)\,dz = n_0 \left(\frac{z}{z_0}\right)^2 e^{-(z/z_0)\beta}, \tag{16}$$

with $(1/n_0) = [z_0\Gamma(3/\beta)]/\beta$ and z_0 a parameter depending on β and the median redshift of the sample. For $\beta = 3/2$ $z_0 = z_{med}/1.406$.

At this point, one might be tempted to directly correlate this quantity with the distribution of matter in the Universe. Things, however, are not quite so simple, as our data is both affected by observational limits and lacking with regards to Dark Matter (DM), which makes up the majority of the matter content in the Universe. This ignorance is accounted for in LSS studies by means of the bias parameters.

3.2.1 Galaxy Bias

Of the Large Scale Structure, we can only directly observe those parts which interact with the electromagnetic spectrum, in other words its barionic matter component. Since, unlike dark matter, baryons are characterized at the current epoch by relevant interactions, the relation between baryon and DM density, and therefore that between DM density and galaxy counts, is not yet understood. This is represented by the relation

$$\frac{\Delta n}{\langle n \rangle} = b \frac{\Delta \rho}{\langle \rho \rangle}, \tag{17}$$

where b is the so called galaxy bias (or clustering bias) parameter, which can depend on a number of variables (like the time and the scales considered). In most cases, though, the assumption of linear bias is a good approximation, and even though the value of b is expected to be scale dependent on small scales (where non linear bias contributions could also be relevant), on large scales we can consider the galaxy bias parameter as fixed, and just for simplicity we will set it equal to unity throughout the rest of this work.

3.2.2 Evolution and Magnification Bias

One of the basic results of general relativity is that photons interact gravitationally, and therefore do not necessarily travel along a straight line. When observing an object through a gravitational field then, the resulting image may appear magnified, distorted or multiplied. This phenomenon is known as gravitational lensing, and can modify the observed source counts by magnifying the light from a source otherwise too weak to be observed and vice versa. We model this uncertainty by means of the magnification bias [77]

$$s\left(z, m_{lim}\right) \equiv \left. \frac{\partial \log_{10} \bar{n}\left(z, L > L_{lim}\right)}{\partial m} \right|,$$

where m is the magnitude of the galaxies considered and $\bar{n}\left(z, L > L_{lim}\right)$ is the average number density of galaxies with luminosity above L_{lim}, which is in turn the minimum luminosity above which a galaxy will be observed.

Moreover, we need to take into account the fact that, during the evolution of the Universe, new galaxies form (or merge) over time, which means their number density does not trivially evolve like a^{-3}. The parameter characterising these deviations is the evolution bias, which is given by

$$f_{evo}\left(z, m_{lim}\right) \equiv \frac{\partial \ln \left[a^3 \bar{n}\left(z, L > L_{lim}\right)\right]}{\partial \ln a},$$

where a is the scale factor.

To simplify our calculations, in the following we will assume that $f_{evo}(\eta)$ is zero, while for the magnification bias parameter we will assume $s(\eta) \simeq 0.4$, which is very close to the estimated value for an Euclid-like survey when redshift values $0.8 \lesssim z \lesssim 1.2$ are considered [77].

3.3 Galaxy bispectrum and nonlinear structure formation

Gravitational phenomena are by nature non linear, and therefore generate non-Gaussianities even when starting from Gaussian initial conditions. In the case of galaxy surveys this is more pronounced than in the case of the CMB because of the longer evolution of the anisotropies (the CMB gives us a picture of the Universe at the time of hydrogen recombination, while the observed galaxies are far more recent). In fact, a galaxy cluster will generally have a density around *one thousand* times greater than the average value for cosmic material [89], a configuration well beyond the linear regime and its hypothesis of small perturbations.

While the highly non-linear regime will probably remain beyond the capabilities of perturbation theory, it is natural, at least in the weakly non-linear case, to study the galaxy count bispectrum, even more than in the CMB case, and such a study has in fact been ongoing for roughly thirty years [56, 72, 75]. Since the distribution of galaxies is 3-dimensional, as opposed to the 2-dimensional surface of last scattering, significantly more independent modes can be observed. For this reason we introduce redshift-dependent bispectra and reduced bispectra, defined by

$$B^{l_1 l_2 l_3}_{m_1 m_2 m_3}(z_1, z_2, z_3) = \mathcal{G}^{l_1 l_2 l_3}_{m_1 m_2 m_3} b_{l_1 l_2 l_3}(z_1, z_2, z_3) = \langle a_{l_1 m_1}(z_1)\, a_{l_2 m_2}(z_1)\, a_{l_3 m_3}(z_1)\rangle\,, \tag{18}$$

where each multipole can be evaluated at different redshift.

The galaxy bispectrum is sensitive to the nonlinear mechanics of gravitational clustering, providing useful constraints on Dark Energy models and modified gravity theories, and on the bias relation between galaxies and the underlying dark matter distribution [44, 108].

Additionally, the bispectrum is also sensitive to primordial non-Gaussianities, but such an effect has to be carefully separated from the non-Gaussian contributions due nonlinear bias and from non-Gaussian evolution of perturbations due to gravitational instability.

3.4 The growth function

While the CMB represents a "snapshot" of the Universe at the recombination epoch, the light coming from each galaxy may have a different redshift, corresponding to different cosmic times and different stages in the formation of cosmic structures, which must be taken into account while measuring anisotropies. Due to the nonlinear nature of structure evolution a perturbative approach is used. This is done by means of a growth function $D_+(a)$, solution to the growth equation [105]

$$\frac{d^2}{da^2}D_+(a) + \frac{1}{a}\left(3 + \frac{d\ln H}{d\ln a}\right)\frac{d}{da}D_+(a) = \frac{3}{2a^2}\Omega_m(a)\,D_+(a)\,, \tag{19}$$

obtained by combining the linearized Poisson, Euler and continuity equations.

During the matter domination era both the Dark Energy and the radiation content of the Universe are negligible when compared to matter. This would let us fix $\Omega_m = 1$, which gives us the simple solution $D_+(a) = a$. However, when considering low-redshift objects, which is the case of most surveys currently available, the effects of Dark Energy can no longer be ignored, and the expression for $D_+(a)$ becomes more complex. While an analytical solution has been calculated by Eisenstein [48], it involves elliptic integrals, and it is often preferable to use the approximate solution by Carroll *et al.* [35]

$$D_+(a) = \frac{5\Omega_{0m}}{2}\left[\Omega_{0m}^{4/7} - \Omega_\Lambda + \left(1 + \frac{\Omega_{0m}}{2}\right)\left(1 + \frac{\Omega_\Lambda}{70}\right)\right]^{-1}. \tag{20}$$

At first order the growth of density perturbations can then be written simply as

$$\delta_m(\mathbf{k}, a) = D_+(a)\,\delta_m(\mathbf{k}, 1)\,. \tag{21}$$

If we set $b = 1$, we can apply this expression to galaxy count densities as

$$\delta_g(\mathbf{k}, a) = D_+(a)\,\delta_g(\mathbf{k}, 1)\,. \tag{22}$$

To obtain higher order solutions in a Newtonian approach we perform a perturbative expansion in the density terms

$$\delta_g(\mathbf{k}, a) = D_+(a)\,\delta_g(\mathbf{k}) + D_+^2(a)\,\delta_g^{(2)}(\mathbf{k}) + \cdots\,, \tag{23}$$

where the $\delta_g^{(n)}(\mathbf{k}, a)$ terms can be expressed in terms of the starting linear perturbations $\delta_g^{(n)}(\mathbf{k})$as

$$\delta_g^{(n)}(\mathbf{k}, a) = \int d^3\mathbf{k}_1 \ldots \int d^3\mathbf{k}_n \delta_D(\mathbf{k} - \mathbf{k_1} - \ldots - \mathbf{k_n})\,F_n(\mathbf{k}_1 \ldots \mathbf{k}_n)\,\delta_g^{(1)}(\mathbf{k}_1) \ldots \delta_g^{(1)}(\mathbf{k}_n)\,, \tag{24}$$

where the $F_n(\mathbf{k}_1 \ldots \mathbf{k}_n)$ are the n-th order perturbation theory kernels.

When using just a Newtonina approach, the second-order kernel which we will use is a well-known result [89].

$$F_2\left(\mathbf{k}_1,\mathbf{k}_2\right)=\frac{5}{7}+\frac{1}{2}\frac{\mathbf{k}_1\cdot\mathbf{k}_2}{k_1k_2}\left(\frac{k_1}{k_2}+\frac{k_2}{k_1}\right)+\frac{2}{7}\frac{\left(\mathbf{k}_1\cdot\mathbf{k}_2\right)^2}{k_1^2k_2^2}. \tag{25}$$

4 CMB-Galaxy Cross-Correlation

Even on large scales the ISW effect is relatively weak and its signal is masked by cosmic variance to the point of making its direct detection in the CMB power spectrum difficult if not impossible. However, as a secondary CMB anisotropy, the integrated Sachs-Wolfe effect is due to the interaction of last-scattering photons with the gravitational potentials they cross, in particular to the net redshift (or blueshift) caused by the evolution of the gravitational potentials the photons go through. . Since these gravitational potentials are generated by the matter distribution in the Universe, (in the Newtonian approximation, through the Poisson equation $\nabla^2\phi=4\pi\delta_\rho\bar{\rho}$), the ISW signal is correlated to the Large Scale Structure, of which the Galaxy distribution is a (biased) tracer. It is therefore possible to define a *two-point cross-correlation function* between ISW generated anisotropies and projected galaxy count anisotropies

$$\xi_G^{ISW}\left(\hat{n}-\hat{n}'\right)=\left\langle\delta_T^{ISW}\left(\hat{n}\right)\delta_G\left(\hat{n}'\right)\right\rangle, \tag{26}$$

and its corresponding power spectrum, which can be defined in terms of the angular coefficients C_l as

$$C_l^{ISW-G}\left(z\right)=\frac{1}{4\pi^4}\int dk P_G^{ISW}(k)\Delta_l^{ISW}(k)\Delta_l^G(k), \tag{27}$$

with $P_G^{ISW}(k)$ the cross-power spectrum of the initial perturbations, and $\Delta_l^{ISW}(k)$ and $\Delta_l^G(k)$ the first order transfer function for ISW anisotropies and for galaxy counts, respectively.

As CMB measurements and galaxy surveys have largely uncorrelated noise sources and systematics, their cross-correlation is a powerful tool to significantly increase the signal-to-noise ratio of the ISW effect. Moreover, both in the ΛCDM model and in most of its variants, the ISW effect is the only non-negligible source of CMB-Galaxy cross-correlation, further simplifying detection [52].

Such an approach, first proposed by Crittenden and Turok in 1994 [42], has been subject of an intensive, twenty years long (and still ongoing) study (see e.g. [47, 49, 55, 92, 83] and references

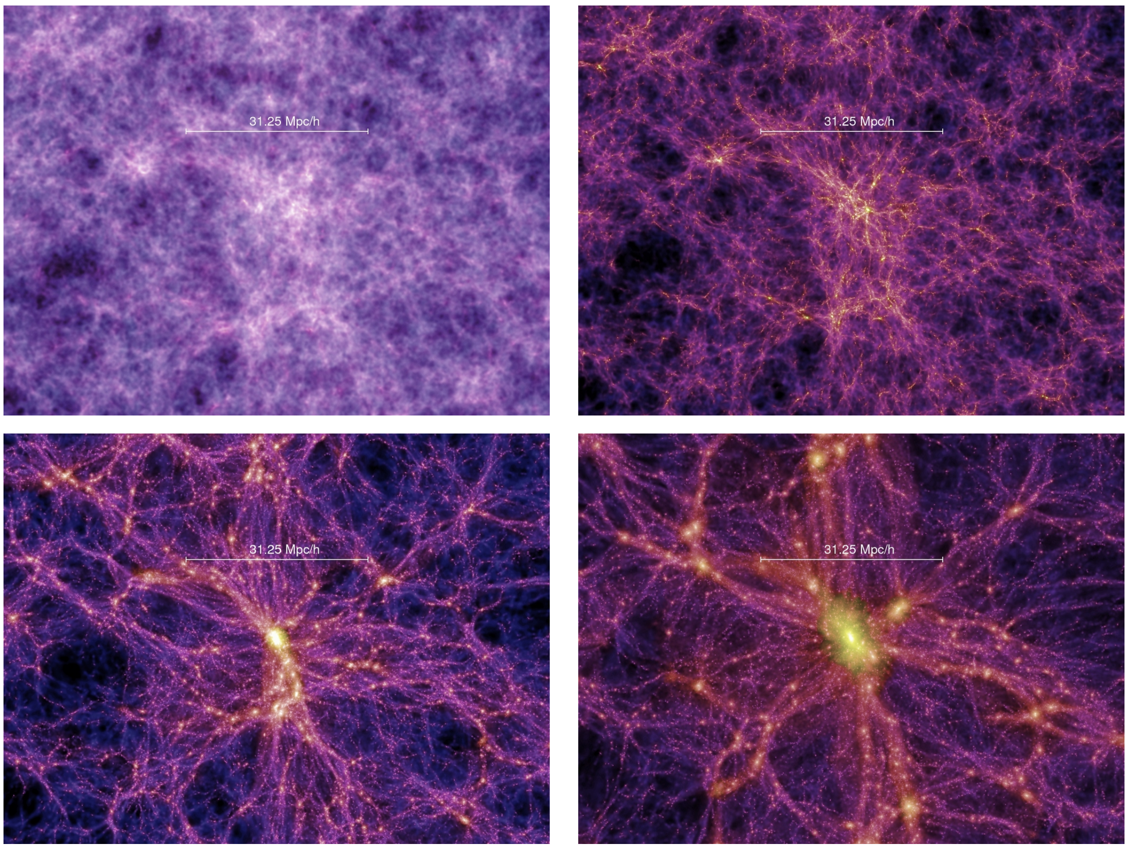

Figure 7: A few images from the "Millennium Run" N-body simulation of LSS evolution. Each snapshot shows the density field in a 15 MPc/h thick slice of space examined at different redshifts (from left to right and top to bottom: $z = 18.3$, $z = 5.7$, $z = 1.4$ and $z = 0$). Purple represents dark matter, while the yellow dots are galaxies and galaxy clusters. (source: *http://wwwmpa.mpa-garching.mpg.de/millennium/*)

therein) which eventually resulted in multiple ISW detection claims with significance up to 4σ (among which [50, 53, 58], see also [9]).

It is therefore advisable, when considering even smaller, second order corrections in the perturbations to the ISW effect and the search for a related non-Gaussian signal, to once again resort to the ISW-Galaxy cross correlation method. Since in this case we are going beyond linear perturbation theory, the lowest-order statistics which might be relevant is a bispectrum between the CMB ISW effect and the Galaxy number counts (with the possibility of various mixed bispectra). Such an approach has in fact been suggested by Schäfer (2008) [61], who studied the signal to noise bispectra and trispectra for a cross-correlation of Planck CMB data with an Euclid-like survey. In a follow-up paper [92] he found a quite low signal-to-noise ratio (≤ 0.828 for the bispectrum) and reached the conclusion that primordial non-Gaussianities would most likely mask those generated by the Rees-Sciama effect, making detection of the latter unlikely.

Such an analysis, however, is based on a few key assumptions - the most important of which is that any cross-correlation has been perfomed in the small-scale Newtonian limit, where general relativistic effects would be negligible.

5 Relativistic effects

In the analysis of CMB-Galaxy cross-correlation, it has become customary in the literature to resort to a Newtonian approximation. This has been justified by the fact that General Relativistic corrections only become relevant on scales of the order of the Horizon, and while it is exactly there that the ISW term dominates, such scales have long been outside the scope of *galaxy* surveys, limiting any study to smaller scales, which are adequately described by Newtonian Gravitation.

Recent experiments however, both ongoing [12, 13, 40] and planned [5, 34] are beginning to probe near-horizon scales, allowing for a study of CMB-ISW cross-correlation at lower multipoles [17, 29, 83]. It is therefore reasonable to ask ourselves whether the Newtonian approximation can still be considered good enough (in the sense that any deviation is masked by the cosmic variance) or if general relativistic effects become significant enough to be potentially detected by present or future surveys [17]. In the latter case, such terms would not only provide (as we will see below) a way to measure primordial non-Gaussianity, but they would constitute powerful probes of the behavior of gravity at very large scales, providing an useful tool to test the limits of (and detect or constrain the possible deviations from) Einstein's General Relativity.

While fully relativistic calculations for the linear ISW effect exist, a study of second-order terms wasn't performed until very recently, which posed limits to studies of the bispectrum. On the face of it, this doesn't seem to pose a problem, as Newtonian calculations predicted the Rees-Sciama effect to be subdominant for low multipoles. However, we will see that this is not the case for a fully relativistic expression.

6 The Second-order CMB Radiation Transfer Function

As the first-order radiation transfer function (or RTF, for short) is insensitive to nonlinear secondary anisotropies, such as the Rees-Sciama effect it is necessary to use perturbation theory up to second order. Extensive calculations and studies have been performed using the Newtonian approximation, but a fully relativistic, second-order transfer function for CMB anisotropies has been calculated , and its effect on the mixed ISW-Galaxy bispectrum has yet to be object of study.

In this section we will rederive the expression for the second-order RTF for low k (i.e. large scales) calculated in [24] - with special attention to those terms which are not negligible for low k, before considering their effect on pure ISW and mixed ISW-Galaxy bispectra in Section 7.

6.1 Evolution of the gravitational potentials

We consider a spatially flat Universe filled with CDM and a cosmological constant Λ (and baryons), with an energy-momentum tensor $T^{\mu}_{\nu} = \rho u^{\mu} u_{\nu}$. We will use the Poisson gauge in our calculations. using conformal time ($d\eta = \frac{dt}{a}$) we can write the perturbed line element around a spatially flat FRW metric as:

$$ds^2 = a^2(\eta)\left[-(1+2\phi)d\eta^2 + 2\omega_i d\eta dx^i + \left[(1-2\psi)\delta_{ij} + \chi_{ij}\right] dx^i dx^j\right]. \tag{28}$$

In the Poisson gauge ω_i is a pure vector mode $\partial^i \omega_i = 0$ while χ_{ij} is a tensor mode (it is divergence-free and traceless $\partial^i \chi_{ij} = 0,\ \chi^i_{\ i} = 0$. We can expand each perturbation quantity into a first-order and a second-order term.

$$\rho(\eta, \mathbf{x}) = \bar{\rho}(\eta)\left(1 + \delta_1 + \frac{\delta_2}{2}\right), \quad v^{\mu} = v^{\mu}_1 + \frac{v^{\mu}_2}{2}, \quad \phi = \phi_1 + \frac{\phi_2}{2}. \tag{29}$$

The Friedmann background equations are

$$3H^2 = a^2(8\pi G\bar{\rho} + \Lambda) \quad \bar{\rho}' = -3H\bar{\rho}. \tag{30}$$

From the analysis of linear perturbations we know that the traceless part of the $(i-j)$ components of Einstein Equations gives $\phi_1 = \psi_1 \equiv \varphi$ and that its trace gives the evolution equation:

$$\varphi'' + 3H\varphi' + a^2\Lambda\varphi = 0. \tag{31}$$

The characteristic equation is$z^2 + 3Hz + a^2\Lambda = 0$, which has solutions $z_\pm = \frac{-3H\pm\sqrt{9H^2-4a^2\Lambda}}{2}$. The two solutions of the differential equation are then

$$\varphi(\mathbf{x}, \eta) = \varphi_0(\mathbf{x}) \exp\left(\frac{-3H \pm \sqrt{9H^2(\eta) - 4a^2(\eta)\Lambda}}{2}\right). \tag{32}$$

With $\varphi_0 = \varphi(\eta_0)$ the gravitational potential extrapolated to the present. We can choose the growing mode solution and rewrite this equation by introducing the growth-suppression factor $g(\eta)$.

$$\varphi(\mathbf{x}, \eta) = g(\eta)\varphi_0(\mathbf{x}). \tag{33}$$

6.1.1 Second-order scalar perturbations

We want to derive the evolution equation for the second-order scalar perturbations of ϕ and ψ, which we will call Φ and Ψ respectively.

The perturbed energy-momentum tensor up to second order for a perfect fluid is, in the pressureless case (and in the Poisson gauge) [22]:

$$T^0{}_0 = -\bar{\rho}\left(1 + \delta_1 + \frac{\delta_2}{2} + v_1^2\right), \tag{34}$$

$$T^i{}_0 = -\bar{\rho}\left(v_1^i + \frac{v_2^i}{2} + (\varphi + \delta_1)\, v_1^i\right), \tag{35}$$

$$T^0{}_0 = -\bar{\rho}\left(v_{1i} + \frac{v_{2i}}{2} + \frac{\omega_{2i}}{2} + (-3\varphi + \delta_1)\, v_{1i}\right), \tag{36}$$

$$T^i{}_j = \bar{\rho} v_1^i v_{1j}, \tag{37}$$

also in the Poisson gauge, $\delta^2 G^i{}_j$ is [21]

$$\frac{1}{a^2}\left(\frac{1}{2}\nabla^2\Phi - \frac{1}{2}\nabla^2\Psi + \frac{a'}{a}\Phi' + 2\frac{a''}{a}\Phi - \left(\frac{a'}{a}\right)^2\Phi + \Psi'' + 2\frac{a'}{a}\Psi' - \frac{1}{2}\partial^i\partial_j(\Phi - \Psi)\right.$$

$$-4\varphi\nabla^2\varphi + 4\left(\frac{a'}{a}\right)^2\varphi^2 - 8\frac{a''}{a}\varphi^2 - 8\frac{a'}{a}\varphi\varphi' - 3\partial_k\varphi\partial^k\varphi + (\varphi')^2$$

$$-\frac{1}{2}\frac{a'}{a}\left(\partial^i\omega_j^{(2)} + \partial_j\omega^{i(2)} - 2\nabla^2\omega^{(2)'}\right) - \frac{1}{4}\left(\partial^i\omega_j^{(2)'} + \partial_j\omega^{i(2)'} - 2\nabla^2\omega^{(2)'}\right) - \frac{1}{4}\nabla^2\chi^{i\,(2)}_{\ j}$$

$$+\frac{1}{4}\chi^{i\,(2)''}_{\ j} + \frac{1}{2}\frac{a'}{a}\chi^{i\,(2)'}_{\ j} + 2 - 3\partial_i\varphi\partial^j\varphi + 4\varphi\partial^i\partial_j\varphi\Bigg), \tag{38}$$

where we have not considered terms of the form $\partial_i\omega^i$ and $\partial^i\chi_{ij}$, which are zero in the Poisson gauge, and neglected linear tensor modes because of their negligible contribution to the bispectrum. We have also neglected linear vector modes, which, according to the standard cosmological models, should not be produced during inflation, and nonlinear tensor modes.

We thus obtain the $(i-j)$ component of the Einstein equations:

$$\Bigg[\Psi'' + H(2\Psi' + \Phi') + \frac{1}{2}\nabla^2(\Phi - \Psi) + (2H' + H^2)\Phi - 4(2H' + H^2)\varphi^2 - \varphi'^2$$

$$-8H\varphi\varphi' - 3(\partial_i\varphi\partial^i\varphi) - 4\varphi\nabla^2\varphi\Bigg]\delta^i_j - \frac{1}{2}\partial^i\partial_j(\Phi - \Psi) - \frac{1}{2}H(\partial^i\omega_{2j} + \partial_j\omega^i_2)$$

$$-\frac{1}{4}(\partial^i\omega'_{2j} + \partial_j\omega^{i'}_2) + \frac{1}{4}(\chi^{i''}_{2j} + 2H\chi^{i'}_{2j} - \nabla^2\chi^i_{2j}) + 2\partial^i\varphi\partial_j\varphi + 4\varphi\partial^i\partial_j\varphi = 8\pi Ga^2\bar{\rho}v^i_1v_{1j}. \tag{39}$$

If we take the traceless part of this equation we obtain:

$$-\left[\frac{1}{6}\nabla^2(\Phi - \Psi) + \frac{2}{3}\nabla\varphi + \frac{4}{3}\varphi\nabla^2\varphi\right]\delta^i_j + \frac{1}{2}\partial^i\partial_j(\Psi - \Phi) + 2\partial^i\varphi\partial_j\varphi + 4\varphi\partial^i\partial_j\varphi$$

$$-\frac{1}{2}H(\partial^i\omega_{2j} + \partial_j\omega^i_2) - \frac{1}{4}(\partial^i\omega'_{2j} + \partial_j\omega^{i'}_2) + \frac{1}{4}(\chi^{i''}_{2j} + 2H\chi^{i'}_{2j} - \nabla^2\chi^i_{2j}) = 8\pi Ga^2\bar{\rho}\left(v^i_1v_{1j} - \frac{1}{3}v_1^2\delta^i_j\right). \tag{40}$$

We can apply the $\partial^i\partial_j$ operator to this equation and, keeping in mind that $\partial_i\omega^i = 0$ and $\partial^i\chi_{ij} = 0$, get rid of vector and tensor modes:

$$\nabla^4(\Psi - \Phi) = -2\partial_i\partial^j\left(\partial^i\varphi\partial_j\varphi\right) + 4\partial_i\partial^j\left(\varphi\partial^i\partial_j\varphi\right) + \frac{4}{3}\nabla^2\left(\varphi\nabla^2\varphi\right)$$

$$+\frac{2}{3}\nabla^2(\nabla\varphi)^2 + 8\pi Ga^2\bar{\rho}\partial_i\partial^j\left(v^i_1v_{1j} - \frac{1}{3}v_1^2\delta^i_j\right). \tag{41}$$

If we define Q as $\nabla^2 Q = -P + 3N$, where P and N are defined in turn by

$$P^i{}_j = 2\partial^i\varphi\partial_j\varphi + 8\pi Ga^2\bar{\rho}v^i_1v_{1j}, \qquad P = P^i{}_i \qquad \nabla^2 N = \partial_i\partial^j P^i{}_j,$$

we get

$$\Psi - \Phi = -4\varphi^2 + Q. \tag{42}$$

The trace of the $(i-j)$ Einstein equation is

$$\Psi'' + H(2\Psi' + \Phi') + \frac{1}{6}\nabla^2(\Phi - \Psi) + \left(2H' + H^2\right)\Phi - 4\left(H' + H^2\right)\varphi^2$$
$$-\varphi'^2 - 8H\varphi\varphi' - (\partial_i\varphi\partial^i\varphi) - \frac{4}{3}\varphi\nabla^2\varphi = \frac{8\pi}{3}Ga^2\bar{\rho}v_1^2, \tag{43}$$

which we can rewrite as

$$\Psi'' + 3H\Psi' + a^2\Lambda\Psi = HQ' + a^2\Lambda Q + N - \varphi'^2 - (\partial_i\varphi\partial^i\varphi). \tag{44}$$

Since we know that

$$v_{1i} = -\frac{1}{4\pi\bar{\rho}a^2G}\partial_i\left(\varphi' + H\varphi\right),$$

we can rewrite $P^i{}_j$ as

$$P^i{}_j = \left(\frac{2}{4\pi\bar{\rho}a^2G}\right)\left[\partial^i\varphi'\partial_j\varphi' + H\left(\partial^i\varphi\partial_j\varphi\right)' + \frac{1}{2}\left(5H - a^2\Lambda\right)\partial^i\varphi\partial_j\varphi\right]. \tag{45}$$

Then $\nabla^2 N$ is equal to

$$\left(\frac{2}{4\pi\bar{\rho}a^2G}\right)\partial_i\partial^j\left[\partial^i\varphi'\partial_j\varphi' + H\left(\partial^i\varphi\partial_j\varphi\right)' + \frac{1}{2}\left(5H - a^2\Lambda\right)\partial^i\varphi\partial_j\varphi\right]. \tag{46}$$

Using the definitions of Q and P we can rewrite $HQ' + a^2\Lambda Q$ as

$$H\left(\nabla^{-2}\left(-P' + 3N'\right)\right) + a^2\Lambda\left(\nabla^{-2}\left(-P + 3N\right)\right), \tag{47}$$

using the definition of N and rearranging the terms we get

$$-\nabla^{-2}\left(HP' + a^2\Lambda P\right) + 3\nabla^{-4}\left(\partial_i\partial^j HP^i{}_j{}' + a^2\Lambda P^i{}_j\right). \tag{48}$$

Using the cosmological background equations and the evolution equation for φ we get

$$
\begin{aligned}
P^{i\,\prime}_{\ j} =& \left(\frac{2}{4\pi\bar{\rho}a^2G}\right)^{\prime}\left[\partial^i\varphi^{\prime}\partial_j\varphi^{\prime} + H\left(\partial^i\varphi\partial_j\varphi\right)^{\prime} + \frac{1}{2}\left(5H^2 - a^2\Lambda\right)\partial^i\varphi\partial_j\varphi\right] \\
&+ \left(\frac{2}{4\pi\bar{\rho}a^2G}\right)\left[\partial^i\varphi^{\prime}\partial_j\varphi^{\prime} + H\left(\partial^i\varphi\partial_j\varphi\right)^{\prime} + \frac{1}{2}\left(5H^2 - a^2\Lambda\right)\partial^i\varphi\partial_j\varphi\right]^{\prime}. \qquad (49)
\end{aligned}
$$

We know that $\bar{\rho}^{\prime} = -3H\bar{\rho}$ and $\frac{a^{\prime}}{a} = H$, which means

$$
\left(\frac{2}{4\pi\bar{\rho}a^2G}\right)^{\prime} = \frac{-2}{4\pi\bar{\rho}^2a^2G}\left(-3H\rho\right) - \frac{4a^{\prime}}{4\pi\bar{\rho}a^3G} = \frac{6H - 4H}{4\pi\bar{\rho}a^3G} = \frac{2}{4\pi\bar{\rho}a^2G}H,
$$

therefore we can now write

$$
\begin{aligned}
P^{i\,\prime}_{\ j} =& \left(\frac{2}{4\pi\bar{\rho}a^2G}\right)\Bigg[H\left(\partial^i\varphi^{\prime}\partial_j\varphi^{\prime}\right) + H^2\left(\partial^i\varphi\partial_j\varphi\right)^{\prime} + \frac{H\left(5H^2 - a^2\Lambda\right)}{2}\partial^i\varphi\partial_j\varphi \\
&+\partial^i\varphi^{\prime\prime}\partial_j\varphi^{\prime} + \partial^i\varphi^{\prime}\partial_j\varphi^{\prime\prime} + H^{\prime}\left(\partial^i\varphi\partial_j\varphi\right)^{\prime} + H\left(\partial^i\varphi^{\prime}\partial_j\varphi + \partial^i\varphi\partial_j\varphi^{\prime}\right)^{\prime} \\
&+\frac{H\left(10H^{\prime} - 2a^2\Lambda\right)}{2}\partial^i\varphi\partial_j\varphi + \frac{\left(5H^2 - a^2\Lambda\right)}{2}\left(\partial^i\varphi\partial_j\varphi\right)^{\prime}\Bigg]. \qquad (50)
\end{aligned}
$$

Rearranging all the terms and using the equations $H^2 + 2H^{\prime} = a^2H$ and $\varphi^{\prime\prime} + 3H\varphi^{\prime} + a^2\Lambda\varphi = 0$ to rewrite the right-hand side of the equation we find

$$
P^{i\,\prime}_{\ j} = \left(\frac{2}{4\pi\bar{\rho}a^2G}\right)\left[-3H\left(\partial^i\varphi^{\prime}\partial_j\varphi^{\prime}\right) - a^2\Lambda H\left(\partial^i\varphi\partial_j\varphi\right) - a^2\Lambda\left(\partial^i\varphi\partial_j\varphi\right)^{\prime}\right]. \qquad (51)
$$

Therefore we can write

$$
\begin{aligned}
HP^{i\,\prime}_{\ j} + a^2\Lambda P^i_{\ j} =& \frac{2}{4\pi\bar{\rho}a^2G}\left[-3H^2\left(\partial^i\varphi^{\prime}\partial_j\varphi^{\prime}\right) - a^2\Lambda H^2\left(\partial^i\varphi\partial_j\varphi\right) - a^2\Lambda H\left(\partial^i\varphi\partial_j\varphi\right)^{\prime}\right] \\
&+\frac{2}{4\pi\bar{\rho}a^2G}\left[\partial^i\varphi^{\prime}\partial_j\varphi^{\prime} + H\left(\partial^i\varphi\partial_j\varphi\right)^{\prime} + \frac{1}{2}\left(5H^2 - a^2\Lambda\right)\partial^i\varphi\partial_j\varphi\right]a^2\Lambda, \qquad (52)
\end{aligned}
$$

and using Friedmann's equations and the evolution equation for φwe get

$$
HP^{i\,\prime}_{\ j} + a^2\Lambda P^i_{\ j} = \left[8\pi\rho a^2G\left(\partial^i\varphi^{\prime}\partial_j\varphi^{\prime}\right) + \left(4\pi\rho a^2G\right)a^2\Lambda\left(\partial^i\varphi\partial_j\varphi\right)\right] \qquad (53)
$$

and we can finally write

$$HP^{i\,\prime}_{\ j} + a^2\Lambda P^i_{\ j} = 2a^2\Lambda\left(\partial^i\varphi\partial_j\varphi\right) - 4\left(\partial^i\varphi'\partial_j\varphi'\right). \tag{54}$$

Then

$$HQ' + a^2\Lambda Q = 3\nabla^{-4}\partial_i\partial^j\left(HP^{i\,\prime}_{\ j} + a^2\Lambda P^i_{\ j}\right) - \nabla^{-2}\left(HP' - a^2\Lambda P\right), \tag{55}$$

is equal to

$$4\left[\nabla^{-2}\left(\partial^i\varphi'\partial_i\varphi'\right) - 3\nabla^{-4}\left(\partial^i\varphi'\partial_j\varphi'\right)\right] - 2a^2\Lambda\left[\nabla^{-2}\left(\partial^i\varphi\partial_i\varphi\right) - 3\nabla^{-4}\left(\partial^i\varphi\partial_j\varphi\right)\right].$$

Keeping in mind that $\varphi = g(\eta)\varphi_0$ we write

$$HQ' + a^2\Lambda Q = \left(4g'^2 - 2a^2\Lambda g^2\right)\left[\nabla^{-2}\left(\partial^i\varphi_0\partial_i\varphi_0\right) - 3\nabla^{-4}\left(\partial^i\varphi_0\partial_j\varphi_0\right)\right]. \tag{56}$$

Using

$$f(\Omega_m) = 1 + \frac{g'(\eta)}{Hg(\eta)}, \tag{57}$$

and Friedmann's equations, we get

$$HQ' + a^2\Lambda Q = 2H^2g^2\left[2\left(f\left(\Omega_m\right) - 1\right) + \frac{8\pi\bar{\rho}a^2G}{H^2} - 3\right]\left[\nabla^{-2}\left(\partial^i\varphi_0\partial_i\varphi_0\right) - 3\nabla^{-4}\left(\partial^i\varphi_0\partial_j\varphi_0\right)\right]. \tag{58}$$

After rearranging some terms

$$HQ' + a^2\Lambda Q = 2H^2g^2\Omega_m\left[\frac{\left(f\left(\Omega_m\right) - 1\right)^2}{\Omega_m} - \frac{3}{\Omega_m} + 3\right]\left[\nabla^{-2}\left(\partial^i\varphi_0\partial_i\varphi_0\right) - 3\nabla^{-4}\left(\partial^i\varphi_0\partial_j\varphi_0\right)\right]. \tag{59}$$

In the same way, for N:

$$N = \nabla^{-2}\left(\partial_i\partial^j P^i_{\ j}\right) = \left\{\partial_i\partial^j\left[\partial^i\varphi_0\partial_j\varphi_0\right]\left((f-1)^2 + 2(f-1) + \frac{1}{2}\left(5 - \frac{a^2\Lambda}{H^2}\right)\right)\right\}, \tag{60}$$

and we find

$$N = \frac{4}{3}g^2\left(\frac{f^2}{\Omega_m}+\frac{3}{2}\right)\nabla^{-2}\left\{\partial_i\partial^j\left[\partial^i\varphi_0\partial_i\varphi_0\right]\right\}. \tag{61}$$

We can then see that

$$P = \frac{4}{3}g^2\left(\frac{f^2}{\Omega_m}+\frac{3}{2}\right)\left[\partial^i\varphi_0\partial_i\varphi_0\right]. \tag{62}$$

And we can finally rewrite the evolution equation for Ψ as:

$$\Psi'' + 3H\Psi' + a^2\Lambda\Psi = HQ' + a^2\Lambda Q + N + \varphi^{'2} - \left(\partial^i\varphi\partial_j\varphi\right) = S(\eta), \tag{63}$$

where

$$S(\eta) = g^2\Omega_m H^2\left[\frac{(f-1)^2}{\Omega_m}\varphi_0^2 + 2\left(2\frac{(f-1)^2}{\Omega_m} - \frac{3}{\Omega_m} + 3\right)\left(\nabla^{-2}\left(\partial^i\varphi_0\partial_i\varphi_0\right) - 3\nabla^{-4}\partial_i\partial^j\left(\partial^i\varphi_0\partial_j\varphi_0\right)\right)\right]$$
$$+g^2\left[\frac{4}{3}\left(\frac{f^2}{\Omega_m}+\frac{3}{2}\right)\nabla^{-2}\partial_i\partial^j\left(\partial^i\varphi_0\partial_j\varphi_0\right) - \left(\partial^i\varphi_0\partial_i\varphi_0\right)\right]. \tag{64}$$

This is a second order differential equation with the solution

$$\Psi(\eta) = \frac{g}{g_m}\Psi_m + \Psi_+(\eta)\int d\eta'\frac{\Psi_-(\eta')}{W(\eta')}S(\eta') - \Psi_-(\eta)\int d\eta'\frac{\Psi_+(\eta')}{W(\eta')}S(\eta'), \tag{65}$$

where $\Psi_+(\eta) = g(\eta)$ and $\Psi_-(\eta) = H(\eta)/a^2(\eta)$ are the solutions of the homogeneous equation and $W(\eta) = \left[H_0^2\left(f_0 + (3\Omega_{0m}/2)\right)\right]/a^3$ is the Wronskian. Given the evolution equation for Ψ, the evolution of the gravitational potential Φ is given by

$$\nabla^4\Psi = \nabla^4\Phi - 4g^2\nabla^4\varphi_0^2 - \frac{4}{3}g^2\left(\frac{f^2}{\Omega_m}+\frac{3}{2}\right)\left[\nabla^2\left(\partial^i\varphi_0\partial_i\varphi_0\right) - 3\partial_i\partial^j\left(\partial^i\varphi_0\partial_j\varphi_0\right)\right], \tag{66}$$

that in the matter-dominated epoch reduces to

$$\nabla^4\Psi_m = \nabla^4\Phi_m - 4g_m^2\nabla^4\varphi_0^2 - \frac{10}{3}g_m^2\left[\nabla^2\left(\partial^i\varphi_0\partial_i\varphi_0\right) - 3\partial_i\partial^j\left(\partial^i\varphi_0\partial_j\varphi_0\right)\right]. \tag{67}$$

since $f(\eta) \to 1$ when $\Omega_m \to 1$ and $\varphi_m = g_m\varphi_0$.

6.1.2 Initial conditions and primordial non-Gaussianity

We now want to discuss the issue of the initial conditions, which we fix at the time when the cosmological parameters relevant today for the LSS and CMB anisotropies are well outside the Hubble radius.

To follow the evolution on super-horizon scales of the density fluctuations we use the curvature perturbation of uniform density hypersurfaces ζ [74]:

$$\zeta = \zeta_1 + \frac{\zeta_2}{2} + ... \qquad \zeta_1 = -\varphi - H\frac{\delta\rho_1}{\bar{\rho}'} \qquad \zeta_2 = -\varphi - H\frac{\delta_2\rho}{\rho'} + \Delta\zeta_2, \tag{68}$$

where

$$\Delta\zeta_2 = 2H\frac{\delta_1\rho}{\rho'}\frac{\delta_1\rho'}{\rho'} + 2\frac{\delta_1\rho}{\rho'}\left(\varphi' + 2H\varphi\right) - \left(\frac{\delta_1\rho}{\rho'}\right)^2\left(H\frac{\rho''}{\rho} - H' - 2H^2\right). \tag{69}$$

We know that ζ remains constant on super-horizon scales, which is why we set the initial conditions after ζ has become constant. In addition, ζ_2 may be reparametrized as $\zeta_2 = 2a_{nl}\left(\zeta_1\right)^2$, where a_{nl} is a parameter related to the primordial non-Gaussianity [23].

Since one of the best tools to potentially detect primordial non-Gaussianity is the analysis of CMB anisotropies we introduce the non-linearity parameter f_{nl}. When $|a_{nl}| \gg 1$, $f_{nl} \simeq \frac{5}{3}a_{nl}$.

At linear order on large scales during the matter-dominated epoch $\zeta_1 = -\frac{5}{3}\varphi_m$, which leads to

$$\zeta_2 = 2a_{nl}\left(\zeta_1\right)^2 = \frac{50}{9}a_{nl}\varphi_m^2 = \frac{50}{9}a_{nl}g_m^2\varphi_0^2. \tag{70}$$

It is possible to express ϕ_m in terms of ζ_2 as [21]

$$\phi_m = -\frac{3}{5}\zeta_2 + \frac{16}{3}\varphi_m^2 + 2\nabla^{-2}\left(\partial^i\varphi_m\partial_i\varphi_m\right) - 6\nabla^{-4}\partial_i\partial^j\left(\partial^i\varphi_m\partial_j\varphi_m\right). \tag{71}$$

Substituting the expression for ζ_2 in the above equation and remembering that $\varphi_m = g_m\varphi_0$ we get

$$\phi_m = -\frac{3}{5}\left(\frac{50}{9}a_{nl}g_m^2\varphi_0^2\right) + \frac{16}{3}g_m^2\varphi_0^2 + 2g_m^2\nabla^{-2}\left(\partial^i\varphi_0\partial_i\varphi_0\right) - 6g_m^2\nabla^{-4}\partial_i\partial^j\left(\partial^i\varphi_0\partial_j\varphi_0\right), \tag{72}$$

rearranging some terms we write

$$\Phi_m = 2g_m^2\left[\left(-1-\frac{5}{3}(a_{nl}-1)\right)-\frac{2}{3}\left(\nabla^{-2}\left(\partial^i\varphi_0\partial_i\varphi_0\right)-3\nabla^{-4}\partial_i\partial^j\left(\partial^i\varphi_0\partial_j\varphi_0\right)\right)\right]. \quad (73)$$

Using the previously found expression for $(\Psi_m - \Phi_m)$ we write

$$\Psi_m = 2g_m^2\left[\left(-1-\frac{5}{3}(a_{nl}-1)\right)+\nabla^{-2}\left(\partial^i\varphi_0\partial_i\varphi_0\right)-3\nabla^{-4}\partial_i\partial^j\left(\partial^i\varphi_0\partial_j\varphi_0\right)\right]. \quad (74)$$

Having found the initial conditions for the two second-order gravitational potentials we can now write the respective evolution equations

$$\begin{aligned}\Psi(\eta) = &\frac{2g(\eta)}{g_m}\left[\varphi_0^2\left(-\frac{5}{3}(a_{nl}-1)-1\right)-\frac{2}{3}\left(\nabla^{-2}\left(\partial^i\varphi_0\partial_i\varphi_0\right)-3\nabla^{-4}\partial_i\partial^j\left(\partial^i\varphi_0\partial_j\varphi_0\right)\right)\right]\\ &+g(\eta)\left[H_0^2\left(f_0-\frac{3}{2}\Omega_{0m}\right)\right]^{-1}\int_{\eta_m}^{\eta}d\eta' H(\eta')a(\eta')S(\eta')\\ &-\frac{H(\eta)}{a^2(\eta)}\left[H_0^2\left(f_0-\frac{3}{2}\Omega_{0m}\right)\right]^{-1}\int_{\eta_m}^{\eta}d\eta' H(\eta')a^3(\eta')S(\eta'),\end{aligned} \quad (75)$$

with $S(\eta)$ given by (8) and

$$\Phi(\eta) = \Psi(\eta)+4g^2(\eta)\varphi_0^2+\frac{4}{3}g^2(\eta)\left(\frac{f^2}{\Omega_m}+\frac{3}{2}\right)\left[\nabla^{-2}\left(\partial^i\varphi_0\partial_i\varphi_0\right)-3\nabla^{-4}\partial_i\partial^j\left(\partial^i\varphi_0\partial_j\varphi_0\right)\right]. \quad (76)$$

Looking over these solutions, we can identify two main contributions: the first term, that proportional to $\nabla^{-2}\left(\partial^i\varphi_0\partial_i\varphi_0\right)-3\nabla^{-4}\partial_i\partial^j\left(\partial^i\varphi_0\partial_j\varphi_0\right)$ contained in $S(\eta)$, is the one responsible for the second order terms in the Newtonian approximation, while the remaining ones represent new, purely relativistic contributions. In Fourier space, the latter are enhanced by a factor of $1/k^2$ with respect to the former, which means that they are relevant on large scales (i.e. low k). In addition, one of these new, relativistic terms depends directly on a_{nl}, and therefore to the amplitude of primordial non-Gaussianity.

6.2 Second order ISW effect

We want to write an expression for the second-order ISW effect, To do so we will consider the large-scale contributions to the equation:

$$\frac{\Delta T}{T}(\hat{n}) = \int_{\eta_m}^{\eta_0} d\eta (\Phi + \Psi)'(\mathbf{x}, \eta)\Big|_{\mathbf{x}=-\hat{\mathbf{n}}(\eta_0-\eta)} + (first - order)^2, \tag{77}$$

we therefore drop from the evolution equations for $\Phi(\eta)$ and $\Psi(\eta)$ the Newtonian terms associated with the Rees-Sciama effect and take the $(first - order)^2$ second-order corrections from the above expression, keeping only the integrated contributions which survive on large scales.

We have then to take the large-scale limit of the following expression [76]:

$$(f.o.)^2 = \int_{\eta^*}^{\eta_0} d\eta \left(4k^{(1)0}\varphi' + 4\varphi'\varphi + 2x^{(1)0}\varphi'' + 2x^{(1)i}\varphi'_{,i}\right) - I_1(\eta^*)(\tau_{1*} + \varphi_* - I_1(\eta^*)), \tag{78}$$

where τ_{1*} is the linear fractional intrinsic temperature perturbation and $I_1(\eta^*)$ is the opposite of the linear ISW effect (with $I_1(\eta) = 2\int_{\eta_0}^{\eta} d\tilde{\eta}\varphi')$. $k^{(1)0}$ and $x^{(1)\mu}$ are respectively the first-order perturbations of the photon wavevector and the background geodesic, with

$$k^{(1)0}(\eta) = -2\varphi + I_1(\eta),$$

$$x^{(1)0}(\eta) = 2\int_{\eta_0}^{\eta} d\tilde{\eta}\left[-\varphi + (\eta - \tilde{\eta})\varphi'\right],$$

$$x^{(1)i}(\eta) = 2\int_{\eta_0}^{\eta_*} d\tilde{\eta}\left[-\varphi e^i + (\eta - \tilde{\eta})\varphi^i\right],$$

where $e^i = -n^i$ is the unit vector which specifies the line-of-sight direction.

Calculating the integrals along the line-of-sight direction and keeping in mind that

$$x^{(1)0} + x^{(1)i}e_i = -2\int_{\eta_0}^{\eta} d\tilde{\eta}\varphi,$$

and

$$2\int_{\eta_0}^{\eta_*} d\eta\varphi' I_1(\eta) = \frac{1}{2}\left[I_1(\eta^*)\right]^2,$$

we get

$$(f.o.)^2 = -4\int_{\eta^*}^{\eta_0} d\eta \left(\varphi\varphi' + \varphi'' \int_{\eta_0}^{\eta} d\tilde{\eta}\varphi\right) + \frac{1}{2}(I_1(\eta^*))^2 - I_1(\eta^*)(\tau_{1*}+\varphi_*) - 4\varphi'_* \int_{\eta^*}^{\eta_0} d\eta(\eta_* - \eta)\varphi. \tag{79}$$

In the following we will use the large-scale solution $\tau_{1*} = -\frac{2\varphi^*}{3}$.

We separate the second-order ISW effect in two parts: early ISW (due to the non-negligible radiation content at last scattering) and late ISW (due to the cosmological constant)

$$\frac{\Delta T_2}{T}(\hat{n}) = \frac{\Delta T_2^{early}}{T} + \frac{\Delta T_2^{late}}{T}. \tag{80}$$

6.2.1 Late ISW

The expression for the Late ISW effect is given by

$$\frac{1}{2}\frac{\Delta T_2^{late}}{T} = \int_{\eta_m}^{\eta_0} d\eta(\Phi+\Psi)'(\mathbf{x},\eta)\bigg|_{\mathbf{x}=-\hat{\mathbf{n}}(\eta_0-\eta)} + (f.o.)^2_{late}. \tag{81}$$

Using the expressions for $\Psi(\eta)$,$\Phi(\eta)$ and the $(f.o.)^2$ term found previously we can write

$$\frac{1}{2}\frac{\Delta T_2^{late}}{T} = \int_{\eta_m}^{\eta_0} d\eta \left[2\left(-1-\frac{5}{3}(a_{nl}-1)\right) g_m g'(\eta) + B'_1(\eta) + 4g(\eta)g'(\eta)\right]\varphi_0^2\bigg|_{\mathbf{x}=-\hat{\mathbf{n}}(\eta_0-\eta)}$$

$$+ \int_{\eta_m}^{\eta_0} d\eta g_m^2 \bar{B}(\eta)\left(\nabla^{-2}\left(\partial^i\varphi_0\partial_i\varphi_0\right) - 3\nabla^{-4}\partial_i\partial^j\left(\partial^i\varphi_0\partial_j\varphi_0\right)\right)\bigg|_{\mathbf{x}=-\hat{\mathbf{n}}(\eta_0-\eta)} + (f.o.)^2_{late}, \tag{82}$$

with

$$B_1(\eta) = \left[H_0^2\left(f_0 - \frac{3}{2}\Omega_{0m}\right)\right]^{-1}\int_{\eta_m}^{\eta} d\tilde{\eta} H^2(\tilde{\eta})\left(f(\tilde{\eta})-1\right)^2 g(\tilde{\eta})a(\tilde{\eta})\left[g(\eta)H(\tilde{\eta}) - g(\tilde{\eta})\frac{a^2(\tilde{\eta})}{a^2(\eta)}H(\eta)\right] \tag{83}$$

$$B_2(\eta) = \left[H_0^2\left(f_0 - \frac{3}{2}\Omega_{0m}\right)\right]^{-1}\int_{\eta_m}^{\eta} d\tilde{\eta} H^2(\tilde{\eta})\left[2\left(f(\tilde{\eta})-1\right)^2 - 3 + 3\Omega_m(\tilde{\eta})\right]\times$$

$$\left[g(\eta)H(\tilde{\eta}) - g(\tilde{\eta})\frac{a^2(\tilde{\eta})}{a^2(\eta)}H(\eta)\right], \tag{84}$$

and

$$\bar{B}(\eta) = \left(\frac{B_2'(\eta)}{g_m^2} - \frac{4}{3}\frac{g'(\eta)}{g_m}\right) + \frac{4}{3}\frac{g'(\eta)g(\eta)}{g_m^2}\left(e(\eta) + \frac{3}{2}\right) + \frac{2}{3}\frac{g^2(\eta)}{g_m^2}e'(\eta), \tag{85}$$

where $e(\eta) = \frac{f^2(\eta)}{\Omega_{m(\eta)}}$ and all the integrals are calculated along the geodesic. We have also dropped from the expressions for $\Psi(\eta)$ and $\Phi(\eta)$ the second-order Newtonian terms, which give a negligible contribution at large scales.

The $(f.o.)^2_{late}$ term is given by

$$-4\int_{\eta_m}^{\eta_0} d\eta \left(\varphi\varphi' + \varphi'' \int_{\eta_0}^{\eta} d\tilde{\eta}\varphi\right) + \frac{1}{2}\left[I_1(\eta_m)\right]^2 - \frac{I_1(\eta_m)\varphi^*}{3}, \tag{86}$$

where

$$\int_{\eta_0}^{\eta} d\tilde{\eta}\varphi = \int_{\eta_0}^{\eta} d\tilde{\eta}\varphi\bigg|_{\mathbf{x}=-\hat{\mathbf{n}}(\eta_0-\eta)} = \int_{\eta_0}^{\eta} d\tilde{\eta} g'(\eta)\varphi_0(\tilde{\eta}, \mathbf{x}). \tag{87}$$

The first term of the $(f.o.)^2_{late}$ contribution can be calculated as seen before, while the other terms have a different dependence on $\hat{\mathbf{n}}$.

Multipoles

The observed CMB anisotropies can be expanded into spherical harmonics with multipoles

$$a_{lm} = \int d^2\hat{n}\frac{\Delta T(\hat{n})}{T}Y^*_{lm}(\hat{n}), \tag{88}$$

the linear and non-linear parts of the temperature fluctuations correspond to a linear Gaussian and a non-Gaussian contribution

$$a_{lm} = a^L_{lm} + a^{NL}_{lm}. \tag{89}$$

At the linear order

$$a_{lm} = 4\pi(-i)^l \int \frac{d^3k}{(2\pi)^3}\phi_{1i}(k)\Delta^{(1)}_l(k)Y^*_{lm}(\hat{k}), \tag{90}$$

where $\phi_{1i}(k)$ are the initial fluctuations and $\Delta_l^{(1)}(k)$ is the linear radiation transfer function, which for the ISW effect on large scales can be written as $j_l(k(\eta_0-\eta_*))/3$. In the following we will take the initial value of the fluctuations in the matter-dominated epoch $\phi_{1i}(\mathbf{k})=\varphi_m(\mathbf{k})$.

For the term proportional to primordial non-Gaussianity

$$A(\hat{n})=\int_{\eta_m}^{\eta_0} d\eta \frac{10}{3}(a_{nl}-1)g_m g'(\eta)\varphi_0^2\Big|_{\mathbf{x}=-\hat{\mathbf{n}}(\eta_0-\eta)},$$

we can Fourier expand it

$$A(\hat{n})=\int \frac{d^3k}{(2\pi)^3}\int_{\eta_m}^{\eta_0} d\eta \mathcal{A} g_m g'(\eta)\left[\varphi_0\right]^2(\mathbf{k})e^{-i\mathbf{k}\cdot\hat{\mathbf{n}}(\eta_0-\eta)},$$

with $\mathcal{A}=-\frac{10}{3}(a_{nl}-1)$ and $\left[\varphi_0\right]^2(\mathbf{k})$ the Fourier transform of $\varphi_0^2(\mathbf{x})$.

Using the Legendre expansion we find

$$A(\hat{n})=\int \frac{d^3k}{(2\pi)^3}\sum_{l=0}^{\infty}(-i)^l(2l+1)\int_{\eta_m}^{\eta_0} d\eta \mathcal{A} g_m g'(\eta) j_l(k(\eta_0-\eta))\left[\varphi_0\right]^2(\mathbf{k})P_l\left(\hat{\mathbf{k}}\cdot\hat{\mathbf{n}}\right). \tag{91}$$

Therefore the non-Gaussian contribution to the multipoles from this term is given by

$$a_{lm}^{NL}(A)=4\pi(-i)^l\int \frac{d^3k}{(2\pi)^3}\int_{\eta_m}^{\eta_0} d\eta \mathcal{A}\frac{g'(\eta)}{g_m}\sum_{l=0}^{\infty}(i)^l j_l(k(\eta_0-\eta))\left[\varphi_0\right]^2(\mathbf{k})4\pi\sum_{m=-l}^{l}Y_{lm}^*(\hat{\mathbf{k}})Y_{lm}(\hat{\mathbf{k}}). \tag{92}$$

Using the orthonormality of spherical harmonics we find

$$a_{lm}^{NL}(A)=4\pi(-i)^l\int \frac{d^3k}{(2\pi)^3}\mathcal{A}\left[\varphi_m\right]^2(\mathbf{k})\left(\int_{\eta_m}^{\eta_0} d\eta\frac{g'(\eta)}{g_m}j_l(k(\eta_0-\eta))\right)Y_{lm}^*(\hat{\mathbf{k}}), \tag{93}$$

with $\mathcal{A}\left[\varphi_m\right]^2(\mathbf{k})$ the convolution

$$\mathcal{A}\left[\varphi_m\right]^2(\mathbf{k})=\frac{1}{(2\pi)^3}\int d^3k_1 d^3k_2\delta\left(k_1+k_2-k\right)\left[-\frac{10}{3}(a_{nl}-1)\right]\varphi_m(\mathbf{k}_1)\varphi_m(\mathbf{k}_2). \tag{94}$$

The remaining terms require similar calculations. For the term

$$\int_{\eta_m}^{\eta_0} d\eta - 2g_m g'(\eta) + B_1'(\eta) + 4g(\eta)g'(\eta), \tag{95}$$

performing the Fourier transform results in

$$\int \frac{d^3k}{(2\pi)^3} \int_{\eta_m}^{\eta_0} \left[d\eta \left(-2g_m g'(\eta) + B_1'(\eta) + 4g_m g'(\eta) \right) [\varphi_0]^2 (\mathbf{k}) \right] e^{-i\mathbf{k}\cdot\hat{\mathbf{n}}(\eta_0 - \eta)}. \tag{96}$$

The Fourier transform of the last term is a bit more complex, due to the presence of the inverse Laplacian operators, and gives us

$$\int \frac{d^3k_1}{(2\pi)^3} \frac{d^3k_2}{(2\pi)^3} \bar{B}(\eta) \left(\frac{\mathbf{k}_1 \cdot \mathbf{k}_2}{k^2} - 3\frac{(\mathbf{k}_1 \cdot \mathbf{k})(\mathbf{k}_2 \cdot \mathbf{k})}{k^4} \right) \varphi_m(\mathbf{k}_1)\varphi_m(\mathbf{k}_2). \tag{97}$$

If we write

$$K_2(\mathbf{k}) = \frac{1}{(2\pi)^3} \int d^3k_1 \int d^3k_2 \bar{B}(\eta) \left(\frac{\mathbf{k}_1 \cdot \mathbf{k}_2}{k^2} - 3\frac{(\mathbf{k}_1 \cdot \mathbf{k})(\mathbf{k}_2 \cdot \mathbf{k})}{k^4} \right) \varphi_m(\mathbf{k}_1)\varphi_m(\mathbf{k}_2), \tag{98}$$

and add together all the terms we find

$$\begin{aligned} \frac{1}{2}\frac{\Delta T_2}{T}(\Phi' + \Psi') = \int \frac{d^3k}{(2\pi)^3} \int_{\eta_m}^{\eta_0} d\eta \Bigg[\Bigg(-\frac{10}{3}(a_{nl} - 1) g_m g'(\eta) - 2g_m g'(\eta) \\ + B_1'(\eta) + 4g(\eta)g'(\eta) \Bigg) [\varphi_0]^2 (\mathbf{k}) - g_m^2 \bar{B}(\eta) K_2(\mathbf{k}) \Bigg] e^{-i\mathbf{k}\cdot\hat{\mathbf{n}}(\eta_0 - \eta)}, \end{aligned} \tag{99}$$

which gives

$$\begin{aligned} a_{lm}^{NL}(\Phi' + \Psi') = 4\pi(-i)^l \int \frac{d^3k}{(2\pi)^3} \int_{\eta_m}^{\eta_0} d\eta j_l(k(\eta_0 - \eta)) \Bigg[\Bigg(-\frac{10}{3}(a_{nl} - 1)\frac{g'(\eta)}{g_m} \\ - \frac{2g'(\eta)}{g_m} + \frac{B_1'(\eta)}{g_m^2} + 4\frac{g(\eta)g'(\eta)}{g_m^2} \Bigg) \Bigg] [\varphi_0]^2 (\mathbf{k}) - \bar{B}(\eta) k_2(\mathbf{k}). \end{aligned} \tag{100}$$

$(\mathbf{First - order})^{\mathbf{2}}$ term

We now take another look at the $(f.o.)^2_{late}$term. Since $\varphi^* \equiv \varphi(\eta_*, \mathbf{x} = -\hat{\mathbf{n}}(\eta_0 - \eta_*))$ and the gravitational potential must be evaluated along the background geodesics, then

$$\int_{\eta_0}^{\eta} d\tilde{\eta}\varphi = \int_{\eta_0}^{\eta} d\tilde{\eta}\varphi\Big|_{\mathbf{x}=-\hat{\mathbf{n}}(\eta_0-\eta_*)} = \int_{\eta_0}^{\eta} d\tilde{\eta} g(\tilde{\eta})\varphi_0(\tilde{\eta},\mathbf{x}). \tag{101}$$

For the integral over $g''(\eta)$:

$$-4\int_{\eta_m}^{\eta_0} d\eta \left(\int d\tilde{\eta}\varphi\right) g''(\eta)\varphi_0(\tilde{\eta},\mathbf{x}), \tag{102}$$

which we can express in terms of its Fourier transform

$$-4\int \frac{d^3k_1}{(2\pi)^3}\frac{d^3k_2}{(2\pi)^3}\int_{\eta_m}^{\eta_0} d\eta \frac{g''(\eta)}{g_m}\int_{\eta_0}^{\eta} d\tilde{\eta}\frac{g(\tilde{\eta})}{g_m}\varphi_m(\mathbf{k}_1)\varphi_m(\mathbf{k}_2)e^{-i\mathbf{k_1}\cdot\hat{\mathbf{n}}(\eta_0-\eta)}e^{-i\mathbf{k_2}\cdot\hat{\mathbf{n}}(\eta_\mathbf{0}-\tilde{\eta})}, \tag{103}$$

using the Rayleigh expansion

$$\begin{aligned}-4\,(4\pi)^2\sum_{L_1M_1}\sum_{L_2M_2}(-i)^{L_1+L_2}Y^*_{L_1M_1}(\hat{\mathbf{n}})Y^*_{L_2M_2}(\hat{\mathbf{n}})\int\frac{d^3k_1}{(2\pi)^3}\frac{d^3k_2}{(2\pi)^3}\int_{\eta_m}^{\eta_0} d\eta\frac{g''(\eta)}{g_m}j_{L_1}(k_1(\eta_0-\eta))\times\\ \int_{\eta_0}^{\eta} d\tilde{\eta}\frac{g(\tilde{\eta})}{g_m}j_{L_2}(k_2(\eta_0-\tilde{\eta}))\varphi_m(\mathbf{k}_1)\varphi_m(\mathbf{k}_2)Y_{L_1M_1}(\hat{\mathbf{n}})Y_{L_2M_2}(\hat{\mathbf{n}}).\end{aligned} \tag{104}$$

Let's now consider the other three terms

$$-4\int_{\eta_m}^{\eta_0} d\eta g(\eta)g'(\eta)\varphi_0^2(\eta,\mathbf{x})\Big|_{\mathbf{x}=-\hat{\mathbf{n}}(\eta_0-\eta)}, \quad \frac{1}{2}\left[I_1(\eta_m)\right]^2, \quad \frac{I_1(\eta_m)\varphi^*}{3}. \tag{105}$$

Fourier transforming the first term gives

$$\int_{\eta_m}^{\eta_0} d\eta g(\eta)g'(\eta)\left[\varphi_m\right]^2(\mathbf{k})e^{-i\mathbf{k}\cdot\hat{\mathbf{n}}(\eta_\mathbf{0}-\eta)}, \tag{106}$$

while Fourier transforming and then Rayleigh expanding the remaining two terms gives

$$4\int_{\eta_m}^{\eta_0} d\eta\frac{g'(\eta)}{g_m}j_{L_1}(k_1(\eta_0-\eta))\int_{\eta_m}^{\eta_0} d\eta\frac{g'(\eta)}{g_m}j_{L_2}(k_2(\eta_0-\eta_*)), \tag{107}$$

and

$$\frac{2}{3}\int_{\eta_m}^{\eta_0} d\eta \frac{g'(\eta)}{g_m} j_{L_1}(k_1(\eta_0-\eta)) j_{L_2}(k_2(\eta_0-\eta_*)), \tag{108}$$

respectively.

Taking into account all of the terms we can write

$$(f.o.)^2_{late} = -4\int \frac{d^3k}{(2\pi)^3}\int_{\eta_m}^{\eta_0} d\eta g(\eta)g'(\eta)\left[\varphi_m\right]^2(\mathbf{k})e^{-i\mathbf{k}\cdot\hat{\mathbf{n}}(\eta_0-\eta)} + (4\pi)^2\sum_{L_1M_1}\sum_{L_2M_2}(-i)^{L_1+L_2}\times$$

$$Y^*_{L_1M_1}(\hat{\mathbf{k}}_1)Y^*_{L_2M_2}(\hat{\mathbf{k}}_2)\int \frac{d^3k_1}{(2\pi)^3}\frac{d^3k_2}{(2\pi)^3}\varphi_m(\mathbf{k}_1)\varphi_m(\mathbf{k}_2)\Delta_{L_1L_2}(k_1,k_2)Y_{L_1M_1}(\hat{\mathbf{k}}_1)Y_{L_2M_2}(\hat{\mathbf{k}}_2), \tag{109}$$

where

$$\Delta_{L_1L_2}(k_1,k_2) = -4\int_{\eta_m}^{\eta_0} d\eta \frac{g''(\eta)}{g_m} j_{L_1}(k_1(\eta_0-\eta))\int_{\eta_0}^{\eta} d\tilde{\eta}\frac{g(\tilde{\eta})}{g_m} j_{L_2}(k_2(\eta_0-\tilde{\eta}))$$

$$+2\int_{\eta_m}^{\eta_0} d\eta\frac{g'(\eta)}{g_m} j_{L_1}(k_1(\eta_0-\eta))\left[2\int_{\eta_m}^{\eta_0} d\eta\frac{g'(\eta)}{g_m} j_{L_2}(k_2(\eta_0-\eta)) + \frac{1}{3} j_{L_2}(k_2(\eta_0-\eta_*))\right]. \tag{110}$$

Using the Rayleigh equation on the first term and keeping in mind that $\varphi_m = g_m\varphi_0$ and the orthonormality of spherical harmonics we find

$$a^{NL}_{lm}\left[(f.o.)^2_{late}\right] = -4\pi(-i)^l\int\frac{d^3k}{(2\pi)^3}\int_{\eta_*}^{\eta} d\eta j_l(k(\eta_0-\eta))\frac{g(\eta)g'(\eta)}{g_m^2}\left[\varphi_0\right]^2(\mathbf{k})Y^*_{lm}(\hat{\mathbf{k}})$$

$$+(4\pi)^2\sum_{L_1M_1}\sum_{L_2M_2}(-i)^{L_1+L_2}\mathcal{G}^{mM_1M_2}_{lL_1L_2}\int\frac{d^3k_1}{(2\pi)^3}\frac{d^3k_2}{(2\pi)^3}\varphi_m(\mathbf{k}_1)\varphi_m(\mathbf{k}_2)\Delta_{L_1L_2}(k_1,k_2)Y_{L_1M_1}(\hat{\mathbf{k}}_1)Y_{L_2M_2}(\hat{\mathbf{k}}_2), \tag{111}$$

where

$$\mathcal{G}^{mM_1M_2}_{lL_1L_2} = \int d^2\mathbf{n}Y_{L_1M_1}(\hat{\mathbf{n}})Y_{L_2M_2}(\hat{\mathbf{n}}), \tag{112}$$

is the Gaunt integral, and

$$K_n(\mathbf{k}) = \frac{1}{(2\pi)^3}\int d^3k_1d^3k_2\delta^{(3)}(\mathbf{k}_1+\mathbf{k}_2-\mathbf{k})f_n(\mathbf{k}_1,\mathbf{k}_2,\mathbf{k})\varphi_*(\mathbf{k}_1)\varphi_*(\mathbf{k}_2), \tag{113}$$

with

$$f_0\left(\mathbf{k}_1,\mathbf{k}_2,\mathbf{k}\right)=-\frac{5}{3}\left(a_{nl}-1\right)-1 \quad f_1\left(\mathbf{k}_1,\mathbf{k}_2,\mathbf{k}\right)=1 \quad f_2\left(\mathbf{k}_1,\mathbf{k}_2,\mathbf{k}\right)=\frac{3\left(\mathbf{k}_1\cdot\mathbf{k}\right)\left(\mathbf{k}_2\cdot\mathbf{k}\right)}{k^4}-\frac{\mathbf{k}_1\cdot\mathbf{k}_2}{k^2}, \tag{114}$$

and

$$\Delta_l^{0(2)}(k)=2\int_{\eta_m}^{\eta_0}d\eta\frac{g'}{g_m}j_l(k(\eta_0-\eta)). \tag{115}$$

$$\Delta_l^{1(2)}(k)=\int_{\eta_m}^{\eta_0}d\eta\frac{B_1'\left(\eta\right)}{g_m^2}j_l(k(\eta_0-\eta)). \tag{116}$$

$$\Delta_l^{2(2)}(k)=2\int_{\eta_m}^{\eta_0}d\eta\bar{B}\left(\eta\right)j_l(k(\eta_0-\eta)). \tag{117}$$

6.2.2 Early ISW

We consider a Universe filled by both pressureless matter (with energy density ρ_m) and a non-negligible radiation content (with energy density ρ_γ) (We suppose here that the cosmological constant is negligible at the epoch of last scattering).

The growing mode of the gravitational potential is then

$$\varphi=\varphi_*\frac{F\left(\eta\right)}{F_*} \tag{118}$$

where [46]

$$F\left(\eta\right)=1-\frac{H}{a}\int_{a_i}^{a}\frac{da}{H}=\frac{3}{5}+\frac{2}{15y}-\frac{8}{15y^2}-\frac{16}{15y^3}+\frac{16\sqrt{1+y}}{15y^3} \tag{119}$$

and $y=\rho_m/\rho_\gamma\propto a$

The linear early ISW effect is given by

$$a_{lm}^L=4\pi(-i)^l\int\frac{d^3k}{(2\pi)^3}\left[2\int_{\eta_*}^{\eta_m}d\eta\varphi'\left(\mathbf{k},\eta\right)j_l(k(\eta_0-\eta))\right]Y_{lm}^*(\hat{\mathbf{k}}) \tag{120}$$

Since most of the contribution to the early ISW effect comes from near recombination we can write

$$2\int_{\eta_*}^{\eta_m} d\eta\varphi'\left(\mathbf{k},\eta\right) j_l(k(\eta_0-\eta)) \approx 2\varphi\left(\mathbf{k},\eta\right)\big|_{\eta_*}^{\eta_m} j_l(k(\eta_0-\eta_*)) = 2\varphi_*\left(\mathbf{k},\eta\right)\frac{\Delta F}{F_*} j_l(k(\eta_0-\eta_*)) \tag{121}$$

At second order the early ISW effect can be written as

$$\frac{1}{2}\frac{\Delta T_2^{early}}{T} = \int_{\eta_*}^{\eta_m} d\eta(\Phi+\Psi)'(\mathbf{x},\eta)\Bigg|_{\mathbf{x}=-\hat{\mathbf{n}}(\eta_0-\eta)} + (f.o.)^2_{early} \tag{122}$$

where

$$\begin{aligned}(f.o.)^2_{early} = &-4\int_{\eta_*}^{\eta_m} d\eta\left(\varphi\varphi' + \varphi''\int_{\eta_0}^{\eta} d\tilde{\eta}\varphi\right) - 4\varphi_*^{'}\int_{\eta_*}^{\eta_0} d\eta(\eta_*-\eta)\varphi \\ &+\frac{1}{2}\left[I_1(\eta_m,\eta_*)\right]^2 + I_1(\eta_m,\eta_*)I_1(\eta_*) - \frac{I_1(\eta_m,\eta_*)\varphi^*}{3}\end{aligned} \tag{123}$$

with $I_1(\eta_*) = I_1(\eta_m,\eta_*) + I_1(\eta_m)$.

We can use the same approximation as before to write

$$\frac{1}{2}\int_{\eta_*}^{\eta_m} d\eta(\Phi+\Psi)'\left(\mathbf{k},\eta\right) j_l(k(\eta_0-\eta)) \approx \frac{1}{2}(\Phi+\Psi)'\Bigg|_{\eta_*}^{\eta_m} j_l(k(\eta_0-\eta_*)). \tag{124}$$

To find a relation between Φ and Ψ we follow the same steps as in the previously examined case of the matter-dominated epoch but replacing the terms for the density and the velocity of the fluid (while keeping in mind that radiation isn't pressureless)

$$\bar{\rho} = \rho_m + \rho_\gamma, \quad v_1^i = v_{1m}^i + v_{1\gamma}^i.$$

We then find for the energy-momentum tensor at second order

$$\delta_2 T^i{}_j = \left(\frac{w_\gamma}{2}\rho_\gamma\delta_{2\gamma}\right) + \rho_\gamma\left(1+w_\gamma\right) v_{1\gamma}^i v_{j\gamma}^1 + \rho_m v_{1m}^i v_{jm}^1, \tag{125}$$

with $w_\gamma = 1/3$.

From the traceless part of the $(i-j)$ Einstein equations we thus get:

$$-\left[\frac{1}{6}\nabla^2(\Phi-\Psi) + \frac{2}{3}\nabla\varphi + \frac{4}{3}\varphi\nabla^2\varphi\right]\delta_j^i + \frac{1}{2}\partial^i\partial_j(\Psi-\Phi)$$

$$+2\partial^i\varphi\partial_j\varphi+4\varphi\partial^i\partial_j\varphi-\frac{1}{2}H(\partial^i\omega_{2j}+\partial_j\omega_2^i)-\frac{1}{4}(\partial^i\omega_{2j}^{'}+\partial_j\omega_2^{i'})$$

$$+\frac{1}{4}(\chi_{2j}^{i''}+2H\chi_{2j}^{i'}-\nabla^2\chi_{2j}^i)=\frac{3H^2}{\rho}\left(\rho_\gamma\left(1+w_\gamma\right)v_{1\gamma}^iv_{1j\gamma}-\frac{1}{3}\rho_\gamma\left(1+w_\gamma\right)v_{1\gamma}^2+\rho_m v_{1m}^i v_{jm}^1-\frac{1}{3}\rho_m v_{1m}^2\right). \tag{126}$$

We can apply the operator $\partial_i\partial^j$ to both sides of the equation and solve in the same way as before with the same result seen in (33) but with a different definition for ${P^i}_j$

$$ {P^i}_j=2\partial^i\varphi\partial_j\varphi+3H^2\left(1+w_\gamma\right)\frac{\rho_\gamma}{\rho}v_{1\gamma}^iv_{j\gamma}^1+3H^2\frac{\rho_m}{\rho}v_{1m}^iv_{jm}^1 \tag{127}$$

We notice that this expression is the same as the one found in the matter-dominated case except for the substitution of the $\bar{\rho}v_1^iv_j^1$ term with $\rho_\gamma\left(1+w_\gamma\right)v_{1\gamma}^iv_{1j\gamma}+\rho_m v_{1m}^iv_{jm}^1$.

It is easy to see that in this case

$$\partial_i\left(\varphi'+H\varphi\right)=-\frac{3}{2}H^2\left(1+\frac{1}{3}\frac{\rho_\gamma}{\rho}\right)v_1^i, \tag{128}$$

since on large scales $v_{1\gamma}^i=v_{1m}^i=v_1^i$.

Therefore we find for ${P^i}_j$

$$ {P^i}_j=\left(\frac{2}{4\pi\bar{\rho}a^2G}\right)\left(1+\frac{\rho_\gamma}{3\rho}\right)\left[\partial^i\varphi'\partial_j\varphi'+H\left(\partial^i\varphi\partial_j\varphi\right)'+\frac{H^2}{2}\left(5+\frac{\rho_\gamma}{\rho}\right)\partial^i\varphi\partial_j\varphi\right]. \tag{129}$$

If we now use the evolution equation for the linear growing mode of the gravitational potential in the case of adiabatic perturbations

$$\varphi=-F\left(\eta\right)\zeta_1, \tag{130}$$

where ζ_1 for adiabatic perturbations on large scales is constant $\zeta_1=-\varphi_*/F_*$, we get

$$ {P^i}_j=\frac{4}{3H^2}\left(1+\frac{\rho_\gamma}{3\rho}\right)^{-1}\frac{1}{F_*^2}\left[F'^2\left(\eta\right)+2HF'\left(\eta\right)F\left(\eta\right)+\frac{H^2}{2}\left(5+\frac{\rho_\gamma}{\rho}\right)F^2\left(\eta\right)\right]\partial^i\varphi_*\partial_j\varphi_*. \tag{131}$$

$$P=\frac{4}{3}\left(1+\frac{\rho_\gamma}{3\rho}\right)^{-1}\frac{1}{F_*^2}\left[\left(\frac{F'\left(\eta\right)}{H}\right)^2+\frac{2F'\left(\eta\right)F\left(\eta\right)}{H}+\frac{1}{2}\left(5+\frac{\rho_\gamma}{\rho}\right)F^2\left(\eta\right)\right]\partial^i\varphi_*\partial_i\varphi_*. \tag{132}$$

$$\nabla^2 N = \frac{4}{3}\left(1+\frac{\rho_\gamma}{3\rho}\right)^{-1}\frac{1}{F_*^2}\left[\left(\frac{F'(\eta)}{H}\right)^2+\frac{2F'(\eta)\,F(\eta)}{H}+\frac{1}{2}\left(5+\frac{\rho_\gamma}{\rho}\right)F^2(\eta)\right]\partial_i\partial^j\left(\partial^i\varphi_*\partial_i\varphi_*\right). \tag{133}$$

$Q = \nabla^{-2}(-P+3N)$ is therefore equal to

$$-\frac{4}{3}\left(1+\frac{\rho_\gamma}{3\rho}\right)^{-1}\frac{1}{F_*^2}\left[\left(\frac{F'(\eta)}{H}\right)^2+\frac{2F'(\eta)\,F(\eta)}{H}+\frac{1}{2}\left(5+\frac{\rho_\gamma}{\rho}\right)F^2(\eta)\right] \tag{134}$$

$$\times\left[\nabla^{-2}\left(\partial^i\varphi_*\partial_i\varphi_*\right)-3\nabla^{-4}\left(\partial_i\partial^j\left(\partial^i\varphi_*\partial_i\varphi_*\right)\right)\right], \tag{135}$$

reintroducing y we get

$$\left(1+\frac{\rho_\gamma}{3\rho}\right)^{-1}=\left(1+\frac{1}{3(y+1)}\right)^{-1}=\left(\frac{4+3y}{3y+3}\right)^{-1}, \tag{136}$$

which, using the fact that $\frac{d}{d\ln a}=\frac{1}{H}\frac{d}{d\eta}$, lets us rewrite

$$Q=-4\left(\frac{1+y}{4+3y}\right)\frac{1}{F_*^2}\left[\dot{F}^2+2F\dot{F}+\frac{1}{2}\left(5+\frac{1}{y+1}\right)F^2\right]$$
$$\times\left[\nabla^{-2}\left(\partial^i\varphi_*\partial_i\varphi_*\right)-3\nabla^{-4}\left(\partial_i\partial^j\left(\partial^i\varphi_*\partial_i\varphi_*\right)\right)\right], \tag{137}$$

with

$$Q=-\frac{3\tilde{Q}\mathcal{K}}{10F_*^2}, \tag{138}$$

where

$$\tilde{Q}=-4\left(\frac{1+y}{4+3y}\right)\left[\dot{F}^2+2F\dot{F}+\frac{1}{2}\left(5+\frac{1}{y+1}\right)F^2\right], \tag{139}$$

and

$$\mathcal{K}=-\nabla^{-2}\left(\frac{10}{3}\partial^i\varphi_*\partial_i\varphi_*\right)+10\nabla^{-4}\left(\partial_i\partial^j\left(\partial^i\varphi_*\partial_i\varphi_*\right)\right). \tag{140}$$

In the Poisson gauge, the expression for the curvature perturbation ζ_2 is

$$\zeta_2 = -\Psi - H\frac{\delta_2\rho}{\rho'}\Delta\zeta_2, \tag{141}$$

while on large scales the $(0-0)$ Einstein equation gives $3H\left(\Psi + H\Phi\right) = 8G\pi\delta_2 T^0{}_0 + 12H^2\varphi^2 + 3\varphi'^2$, and the second-order corrections $\Delta\zeta_2$ are (69)

The $(0-0)$ component of the energy-momentum tensor is $\delta_2 T^0{}_0 = -\frac{1}{2}\delta_2\rho - \rho_m v_{1m}^2 - \frac{4}{3}\rho_\gamma v_{1\gamma}^2$. Therefore

$$\zeta_2 = \Psi + 2\frac{\rho}{\rho'}\Psi' - 2\frac{\rho}{\rho'}HQ + 2\frac{\rho}{\rho'}H\Psi - \frac{2\varphi'^2\rho}{H\rho'} + \Delta\zeta_2, \tag{142}$$

changing time variable from $\frac{d}{d\eta}$ to $\frac{d}{d\ln a}$ we can see that

$$-\frac{1}{2}\frac{\dot\rho}{\rho}\Psi + \left(\Psi + \dot\Psi\right) = \frac{\sqrt{\rho}}{a}\left[\frac{a}{\sqrt{\rho}}\Psi\right]^{\cdot}, \tag{143}$$

and we get

$$\zeta_2 = 2\frac{\rho}{\dot\rho}\frac{\sqrt{\rho}}{a}\left[\frac{a}{\sqrt{\rho}}\Psi\right]^{\cdot} - 2\frac{\rho}{\dot\rho}Q - 2\frac{\rho}{\dot\rho}\dot\varphi, \tag{144}$$

which leads to

$$\frac{\sqrt{\rho}}{a}\left[\frac{a}{\sqrt{\rho}}\Psi\right]^{\cdot} = \frac{1}{2}\frac{\dot\rho}{\rho}\zeta_2 + \left[\dot\varphi^2 + Q - \frac{1}{2}\frac{\dot\rho}{\rho}\Delta\zeta_2\right]. \tag{145}$$

Now we complete the expression for $\Delta\zeta_2$ in the case of pressureless matter and radiation. We know that $\rho'_\gamma = -4H\rho_\gamma$, $\rho'_m = -3H\rho_m$ and $\rho = \rho_\gamma + \rho_m$

then

$$H\frac{\rho''}{\rho} - H' - 2H^2 = -H^2\left(6 - \frac{3\rho_m}{3\rho_m + 4\rho_\gamma}\right). \tag{146}$$

We can now rewrite $\delta_1\rho$ and $\delta_1\rho'$ in terms of φ using the continuity equation for the total energy and the large-scale limit of the $(0-0)$ Einstein equation

$$\delta_1\rho' = -3H\left(\delta_1\rho + \delta_1 p\right) - 3\left(p + \rho\right)\varphi' = 0. \tag{147}$$

Since the perturbations are adiabatic

$$\frac{\delta_1 \rho_\gamma}{\rho_\gamma} = \frac{4}{3}\frac{\delta_1 \rho_m}{\rho_m}, \tag{148}$$

which, together with the continuity equation gives us

$$\frac{\delta_1 \rho'}{\rho'} = -3H\left[1 + \frac{1}{3}\frac{4\rho_\gamma}{4\rho_\gamma + 3\rho_m}\right]\frac{\delta_1 \rho}{\rho'} - \frac{\varphi'}{H}. \tag{149}$$

Then we can write $\Delta\zeta_2$ as

$$\Delta\zeta_2 = -H^2\left(\frac{\delta_1 \rho}{\rho'}\right)^2\left(1 + \frac{4\rho_\gamma}{4\rho_\gamma + 3\rho_m}\right) + 4H\varphi\frac{\delta_1 \rho}{\rho'}. \tag{150}$$

The $(0-0)$ Einstein equation on large scales is

$$\Delta\zeta_2 = \left[2\frac{\dot\rho}{\rho}\left(\dot\varphi + \varphi\right)\right]^2\left[1 + \frac{1}{3}\frac{4\rho_\gamma}{4\rho_\gamma + 3\rho_m}\right] - 8\frac{\rho}{\dot\rho}\left(\dot\varphi + \varphi\right)\varphi, \tag{151}$$

using the equation (118) we can write

$$-\frac{1}{2}\frac{\dot\rho}{\rho}\Delta\zeta_2 = \frac{1}{F_*^2}\left[2R\dot F^2 - 2(2-R)F^2 - 4(1-R)F\dot F\right]\varphi_*^2, \tag{152}$$

with

$$R = \frac{1+y}{4+3y}\left(1 + \frac{4}{4+3y}\right), \tag{153}$$

integrating the equation for $\frac{\delta_1 \rho'}{\rho'}$ gives us

$$\Psi = -F\left(\eta\right)\zeta_2 + \frac{\sqrt{\rho}}{a}\int_{a_i}^{a}\frac{da}{\sqrt{\rho}}\left[\dot\varphi^2 + Q - \frac{1}{2}\frac{\dot\rho}{\rho}\Delta\zeta_2\right] + c\frac{\sqrt{\rho}}{a}. \tag{154}$$

Therefore

$$\Phi + \Psi = -2F\left(\eta\right)\zeta_2 + \frac{1}{F_*^2}\left[4F^2 + 2\frac{\sqrt{\rho}}{a}\int_{a_i}^{a}\frac{da}{\sqrt{\rho}}\left((1-2R)\dot F^2 + 4(1-R)F\dot F + 2(2-R)F^2\right)\right]\varphi_*^2$$

$$+\frac{3}{10F_*^2}\left(\tilde{Q}-2\frac{\sqrt{\rho}}{a}\int_{a_i}^{a}\frac{da}{\sqrt{\rho}}\tilde{Q}\right)\mathcal{K}. \tag{155}$$

Which leads to the following result for the early ISW effect

$$a_{lm}^{NL}=-4\pi(-i)^l\int\frac{d^3k}{(2\pi)^3}\left[K_0\left(\mathbf{k}\right)\Delta_l^{0(2)}(k)+K_1\left(\mathbf{k}\right)\Delta_l^{1(2)}(k)+K_2\left(\mathbf{k}\right)\Delta_l^{2(2)}(k)\right]Y_{lm}^*(\hat{\mathbf{k}})$$
$$+(4\pi)^2\sum_{L_1M_1}\sum_{L_2M_2}(-i)^{L_1+L_2}\mathcal{G}_{lL_1L_2}^{mM_1M_2}\int\frac{d^3k_1}{(2\pi)^3}\frac{d^3k_2}{(2\pi)^3}\varphi_*(\mathbf{k}_1)\varphi_*(\mathbf{k}_2)\Delta_{L_1L_2}(k_1,k_2)Y_{L_1M_1}(\hat{\mathbf{k}}_1)Y_{L_2M_2}(\hat{\mathbf{k}}_2), \tag{156}$$

with

$$\Delta_l^{0(2)}(k)=\frac{6}{5}\frac{\Delta F}{F_*^2}j_l(k(\eta_0-\eta_*)), \tag{157}$$

$$\Delta_l^{1(2)}(k)=\frac{1}{F_*^2}\left[\frac{\sqrt{\rho}}{a}\int_{a_i}^{a}\frac{da}{\sqrt{\rho}}\left((1-2R)\dot{F}^2+4(1-R)F\dot{F}+2(2-R)F^2\right)\right]\Bigg|_{a_*}^{a_m}j_l(k(\eta_0-\eta_*))$$
$$+\frac{4}{5}\frac{\Delta F}{F_*^2}j_l(k(\eta_0-\eta_*)), \tag{158}$$

$$\Delta_l^{2(2)}(k)=\frac{1}{F_*^2}\left[\frac{\tilde{Q}}{2}-\frac{\sqrt{\rho}}{a}\int_{a_i}^{a}\frac{da}{\sqrt{\rho}}\tilde{Q}\right]\Bigg|_{a_*}^{a_m}j_l(k(\eta_0-\eta_*)), \tag{159}$$

and

$$\Delta_{L_1L_2}(k_1,k_2)=\left(2\frac{\Delta F}{F_*^2}+\frac{2}{3}\frac{\Delta F}{F_*}\right)j_{L_1}(k(\eta_0-\eta_*))j_{L_2}(k(\eta_0-\eta_*))$$
$$+4\frac{\Delta F}{F_*^2}j_{L_2}(k(\eta_0-\eta_*))\int_{\eta_m}^{\eta_0}d\eta\frac{g'(\eta)}{g_m}j_{L_1}(k(\eta_0-\eta))$$
$$-\frac{F'(\eta_*)}{F_*}j_{L_2}(k(\eta_0-\eta_*))\left[\int_{\eta_*}^{\eta_m}d\eta\,(\eta_*-\eta)\,\frac{F(\eta)}{F_*}j_{L_1}(k(\eta_0-\eta_*))+\int_{\eta_m}^{\eta_0}d\eta\frac{g(\eta)}{g_m}j_{L_1}(k(\eta_0-\eta))\right]$$
$$+4\int_{\eta_*}^{\eta_m}d\eta\frac{F''(\eta)}{F_*}j_{L_2}(k(\eta_0-\eta))\left[\int_{\eta}^{\eta_m}d\tilde{\eta}\frac{F(\tilde{\eta})}{F_*}j_{L_1}(k(\eta_0-\tilde{\eta}))+\int_{\eta_m}^{\eta_0}d\tilde{\eta}\frac{g(\tilde{\eta})}{g_m}j_{L_1}(k(\eta_0-\tilde{\eta}))\right]. \tag{160}$$

7 Relativistic corrections for galaxy counts

Galaxy count terms at very large scales are subject to a number of relativistic corrections, which have been calculated at first order [82, 87, 107], while a full calculation of second order terms is in progress [28, 44, 45]. We briefly examine relativistic corrections for first order galaxy counts before discussing which terms are most relevant and when.

7.1 First order corrections for redshift dependent galaxy counts

At first order the relativistic corrections are (for $f\left(z\right)=0$ as set in section 3 and $\phi=\psi=\varphi$) [87]:

$$\delta_{rsd}\left(\mathbf{n},z\right)=\frac{1}{H(z)}\partial_r\left(\mathbf{v}\cdot\mathbf{n}\right), \tag{161}$$

$$\delta_{\mathcal{K}}\left(\mathbf{n},z\right)=\frac{5s\left(z\right)-2}{2}\int_0^{r_s}\frac{r_s-r}{r_s r}\nabla^2\varphi dr, \tag{162}$$

$$\delta_{dopp}\left(\mathbf{n},z\right)=\left[\frac{H'\left(z\right)}{H^2\left(z\right)}+\frac{2-5s\left(z\right)}{r_s H\left(z\right)}+5s\left(z\right)\right]\left(\mathbf{v}\cdot\mathbf{n}\right)+3H\nabla^{-2}\left(\nabla\cdot\mathbf{v}\right), \tag{163}$$

$$\delta_{lp}\left(\mathbf{n},z\right)=\left(5s\left(z\right)-1\right)\varphi\left(z\right)+\frac{\varphi'\left(z\right)}{H\left(z\right)}+\left[\frac{H'\left(z\right)}{H^2\left(z\right)}+\frac{2}{r_s H\left(z\right)}\right]\varphi\left(z\right), \tag{164}$$

$$\delta_{td}\left(\mathbf{n},z\right)=\frac{2-5s\left(z\right)}{r_s}\int_0^{r_s}\varphi dr, \tag{165}$$

$$\delta_{ISW}\left(\mathbf{n},z\right)=2\left[\frac{H'\left(z\right)}{H^2\left(z\right)}+\frac{2}{r_s H\left(z\right)}\right]\int_{\eta_s}^{\eta_0}\varphi' d\eta, \tag{166}$$

where $\mathbf{v}$ is the velocity perturbation (in the longitudinal gauge), $s(z)$ the magnification bias and r_s the comoving distance from the galaxies examined.

The three terms $\delta_{lp}, \delta_{td}, \delta_{ISW}$ (which represent the effects of local potentials, Shapiro time-delay and the galaxy count counterpart to the ISW respectively), depend directly on the gravitational potential, rather than its spatial derivatives, which translates in Fourier space to an additional $(H(z)/k)^2$ factor with respect to redshift and lensing terms. However, modes with $k \ll H(z)$ are not accessible by current or planned near-future surveys because of their low maximum redshift values. In fact, these terms have been estimated not to be detectable with single-tracer surveys with z up to 4 [16]. The term δ_{dopp}, which depends on the first spatial derivatives of the gravitational potential, has a similar behavior, while the dominant contributions are represented by the δ_{rsd} and $\delta_{\mathcal{K}}$ terms, which represent redshift space distortions and lensing convergence respectively.

Considering only the δ_{rsd} and $\delta_{\mathcal{K}}$ terms, we can write down the expression for the relativistic galaxy count multipoles by Fourier transforming the corrections and expanding them in spherical harmonics [36]:

$$a^L_{lm}(z) = 4\pi(-i)^l \int \frac{d^3k}{(2\pi)^3} \Bigg\{ [j_l(k(\eta_0 - \eta)) D_+(z)\, \delta_1(k)] + \left(\frac{kr_s}{H(z)} j''_l(kr_s)\right) + (2s-5)\left[l(l+1)\int dr' \frac{r-r'}{rr'} g(\eta)\, \varphi_m j''_l(kr)\right]\Bigg\} Y^*_{lm}(\hat{\mathbf{k}}). \tag{167}$$

7.2 Projected galaxy counts and Newtonian approximation

Relativistic corrections *do not seem,* on the other hand, to significantly affect correlations between *cumulative* galaxy counts, projected along the line-of-sight, and either galaxy counts or microwave background fluctuations. Non-integrated effects on both galaxy and mixed power spectra appear to be strongly suppressed when cumulative galaxy counts are considered , leaving $\delta_{\mathcal{K}}$ as the only significant relativistic contribution, which itself goes to zero if a magnification bias $s(z) \simeq 0.4$ is considered [36, 107].

Under these conditions, limiting our calculation of the *projected* galaxy counts to the Newtonian terms seems acceptable. Of course, this assumes that relativistic corrections *at both first and second order* remain marginal with respect to the *second order* density perturbations when cumulative galaxy counts are considered. This seems reasonable, but has not been studied as of yet, and should not be taken for granted. A truly complete calculation at second-order in the cosmological perturbations will be possible only once the effect of all relativistic contributions on cumulative galaxy counts is considered.

8 The mixed Galaxy-ISW bispectrum

Using perturbation theory up to second-order at the tree level, the expression for the bispectrum reduces to [99]

$$B^{l_a l_b l_c}_{m_a m_b m_c} = \left\langle a^{NL}_{l_a m_a} a^L_{l_b m_b} a^L_{l_c m_c} + permutations \right\rangle. \tag{168}$$

(In the following, when considering mixed bispectra, we will rename the multipole coefficients relative to galaxy counts as $\gamma_{lm}(z)$ and those relative to temperature anisotropies as $\tau_{lm}(z)$ for ease of notation.)

The $\langle\tau\tau\gamma\rangle$ bispectrum is then made up by the following terms

$$\left\langle \tau^{NL}_{l_am_a}\tau^{L}_{l_bm_b}\gamma^{L}_{l_cm_c}(z)+\tau^{L}_{l_am_a}\tau^{NL}_{l_bm_b}\gamma^{L}_{l_cm_c}(z)+\tau^{L}_{l_am_a}\tau^{L}_{l_bm_b}\gamma^{NL}_{l_cm_c}(z)\right\rangle . \tag{169}$$

while for the $\langle\tau\gamma\gamma\rangle$ bispectrum

$$\left\langle \tau^{NL}_{l_am_a}\gamma^{L}_{l_bm_b}(z)\,\gamma^{L}_{l_cm_c}(z)+\tau^{L}_{l_am_a}\gamma^{NL}_{l_bm_b}(z)\,\gamma^{L}_{l_cm_c}(z)+\tau^{L}_{l_am_a}\gamma^{L}_{l_bm_b}(z)\,\gamma^{NL}_{l_cm_c}(z)\right\rangle . \tag{170}$$

Before writing down the terms for the mixed bispectra, we provide a brief summary of all the multipole terms used: both the first and second order terms for the integrated Sachs-Wolfe effect and cumulative galaxy counts, and those for redshift-dependent galaxy counts up to linear order.

8.1 Multipole terms - ISW

For large-scale ISW anisotropies at linear order

$$\tau^{L}_{lm}=4\pi(-i)^l\int\frac{d^3k}{(2\pi)^3}\left[\frac{j_l(k(\eta_0-\eta_*))}{3}\varphi_m(k)\right]Y^*_{lm}(\hat{\mathbf{k}}). \tag{171}$$

At second order, by adding together the Sachs-Wolfe, Early ISW and late ISW terms calculated previously we get

$$\tau^{NL}_{lm}=4\pi(-i)^l\int\frac{d^3k}{(2\pi)^3}\left[K_0(\mathbf{k})\,\Delta^{0(2)}_l(k)+K_1(\mathbf{k})\,\Delta^{1(2)}_l(k)+K_2(\mathbf{k})\,\Delta^{2(2)}_l(k)\right]Y^*_{lm}(\hat{\mathbf{k}})$$
$$+(4\pi)^2\sum_{L_1M_1}\sum_{L_2M_2}(-i)^{L_1+L_2}\mathcal{G}^{mM_1M_2}_{lL_1L_2}\int\frac{d^3k_1}{(2\pi)^3}\frac{d^3k_2}{(2\pi)^3}\varphi_*(\mathbf{k}_1)\varphi_*(\mathbf{k}_2)\Delta_{L_1L_2}(k_1,k_2)Y_{L_1M_1}(\hat{\mathbf{k}}_1)Y_{L_2M_2}(\hat{\mathbf{k}}_2), \tag{172}$$

where

$$K_n(\mathbf{k})=\frac{1}{(2\pi)^3}\int d^3k_1d^3k_2\delta^{(3)}(\mathbf{k}_1+\mathbf{k}_2-\mathbf{k})\,f_n(\mathbf{k}_1,\mathbf{k}_2,\mathbf{k})\,\varphi_*(\mathbf{k}_1)\varphi_*(\mathbf{k}_2), \tag{173}$$

with

$$f_0\left(\mathbf{k}_1,\mathbf{k}_2,\mathbf{k}\right)=-\frac{5}{3}\left(a_{nl}-1\right)-1\quad f_1\left(\mathbf{k}_1,\mathbf{k}_2,\mathbf{k}\right)=1\quad f_2\left(\mathbf{k}_1,\mathbf{k}_2,\mathbf{k}\right)=\frac{3\left(\mathbf{k}_1\cdot\mathbf{k}\right)\left(\mathbf{k}_2\cdot\mathbf{k}\right)}{k^4}-\frac{\mathbf{k}_1\cdot\mathbf{k}_2}{k^2},\tag{174}$$

and where

$$\Delta_l^{0(2)}(k)=\left(\frac{1}{3}+\frac{6}{5}\frac{\Delta F}{F_*^2}\right)j_l(k(\eta_0-\eta_*))+2\int_{\eta_m}^{\eta_0}d\eta\frac{g'}{g_m}j_l(k(\eta_0-\eta))\tag{175}$$

$$\Delta_l^{1(2)}(k)=\left\{\frac{7}{18}+\frac{4}{5}\frac{\Delta F}{F_*^2}+\frac{1}{F_*^2}\left[\frac{\sqrt{\rho}}{a}\int_{a_i}^{a}\frac{da}{\sqrt{\rho}}\left((1-2R)\dot{F}^2+4(1-R)F\dot{F}+2(2-R)F^2\right)\right]\Bigg|_{a_*}^{a_m}\right\}j_l(k(\eta_0-\eta_*))$$
$$+\int_{\eta_m}^{\eta_0}d\eta\frac{B_1'(\eta)}{g_m^2}j_l(k(\eta_0-\eta))\tag{176}$$

$$\Delta_l^{2(2)}(k)=\left\{-\frac{1}{3}+\frac{1}{F_*^2}\left[\frac{\tilde{Q}}{2}-\frac{\sqrt{\rho}}{a}\int_{a_i}^{a}\frac{da}{\sqrt{\rho}}\tilde{Q}\right]\Bigg|_{a_*}^{a_m}\right\}j_l(k(\eta_0-\eta_*))+2\int_{\eta_m}^{\eta_0}d\eta\bar{B}\left(\eta\right)j_l(k(\eta_0-\eta)),\tag{177}$$

and

$$\begin{aligned}\Delta_{L_1L_2}(k_1,k_2)=&-4\int_{\eta_m}^{\eta_0}d\eta\frac{g''(\eta)}{g_m}j_{L_1}(k_1(\eta_0-\eta))\int_{\eta_0}^{\eta}d\tilde{\eta}\frac{g(\tilde{\eta})}{g_m}j_{L_2}(k_2(\eta_0-\tilde{\eta}))\\&+2\int_{\eta_m}^{\eta_0}d\eta\frac{g'(\eta)}{g_m}j_{L_1}(k_1(\eta_0-\eta))\left[2\int_{\eta_m}^{\eta_0}d\eta\frac{g'(\eta)}{g_m}j_{L_2}(k_2(\eta_0-\eta))+\frac{1}{3}j_{L_2}(k_2(\eta_0-\eta_*))\right]\\&+\left(2\frac{\Delta F}{F_*^2}+\frac{2}{3}\frac{\Delta F}{F_*}\right)j_{L_1}(k(\eta_0-\eta_*))j_{L_2}(k(\eta_0-\eta_*))+4\frac{\Delta F}{F_*^2}j_{L_2}(k(\eta_0-\eta_*))\int_{\eta_m}^{\eta_0}d\eta\frac{g'(\eta)}{g_m}j_{L_1}(k(\eta_0-\eta))\\&-\frac{F'\left(\eta_*\right)}{F_*}j_{L_2}(k(\eta_0-\eta_*))\left[\int_{\eta_*}^{\eta_m}d\eta\left(\eta_*-\eta\right)\frac{F(\eta)}{F_*}j_{L_1}(k(\eta_0-\eta_*))+\int_{\eta_m}^{\eta_0}d\eta\frac{g(\eta)}{g_m}j_{L_1}(k(\eta_0-\eta))\right]\\&+4\int_{\eta_*}^{\eta_m}d\eta\frac{F''(\eta)}{F_*}j_{L_2}(k(\eta_0-\eta))\left[\int_{\eta}^{\eta_m}d\tilde{\eta}\frac{F(\tilde{\eta})}{F_*}j_{L_1}(k(\eta_0-\tilde{\eta}))+\int_{\eta_m}^{\eta_0}d\tilde{\eta}\frac{g(\tilde{\eta})}{g_m}j_{L_1}(k(\eta_0-\tilde{\eta}))\right].\end{aligned}\tag{178}$$

8.2 Multipole terms - Galaxy Counts

Using Eulerian perturbation theory in the Newtonian approximation we find [61, 89]:

$$\gamma_{lm}^{L}\left(z\right)=4\pi(-i)^{l}\int\frac{d^{3}k}{(2\pi)^{3}}\left[j_{l}(k(\eta_{0}-\eta))D\left(z\right)\delta_{1}(\mathbf{k})\right]Y_{lm}^{*}(\hat{\mathbf{k}}),\tag{179}$$

at linear order and

$$\gamma_{lm}^{NL}\left(z\right)=-4\pi(-i)^{l}\int\frac{d^{3}k}{(2\pi)^{3}}\left[\delta_{2}\left(\mathbf{k}\right)D_{+}^{2}\left(z\right)\right]Y_{lm}^{*}(\hat{\mathbf{k}}),\tag{180}$$

at second order, with

$$\delta_{2}\left(\mathbf{k}\right)=\frac{1}{(2\pi)^{6}}\int d^{3}k_{1}d^{3}k_{2}\delta_{D}^{(3)}\left(\mathbf{k}_{1}+\mathbf{k}_{2}-\mathbf{k}\right)F_{2}\left(\mathbf{k}_{1},\mathbf{k}_{2},\mathbf{k}\right)\delta_{1}(\mathbf{k}_{1})\delta_{1}(\mathbf{k}_{2}),\tag{181}$$

and

$$F_{2}\left(\mathbf{k}_{1},\mathbf{k}_{2},\mathbf{k}\right)=\frac{5}{7}+\frac{1}{2}\frac{\mathbf{k}_{1}\cdot\mathbf{k}_{2}}{k_{1}k_{2}}\left(\frac{k_{1}}{k_{2}}+\frac{k_{2}}{k_{1}}\right)+\frac{2}{7}\frac{\left(\mathbf{k}_{1}\cdot\mathbf{k}_{2}\right)^{2}}{k_{1}^{2}k_{2}^{2}},$$

at second order.

8.2.1 Projected galaxy counts

For cumulative galaxy counts projected along the line-of-sight, we resort to the Newtonian approximation, and, following the results in [61, 92], we find

$$\gamma_{lm}^{L}=4\pi(-i)^{l}\int\frac{d^{3}k}{(2\pi)^{3}}\left[j_{l}(k(\eta_{0}-\eta))\int_{0}^{\eta_{H}}n(z)\frac{dz}{d\eta}D_{+}\left(\eta\right)\delta_{1}(\mathbf{k})\right]Y_{lm}^{*}(\hat{\mathbf{k}}),\tag{182}$$

at linear order, and

$$\gamma_{lm}^{NL}=4\pi(-i)^{l}\int\frac{d^{3}k}{(2\pi)^{6}}\left[j_{l}(k(\eta_{0}-\eta))\int_{0}^{\eta_{H}}n(z)\frac{dz}{d\eta}j_{l}(k(\eta_{0}-\eta))D_{+}^{2}\left(\eta\right)\delta_{2}(\mathbf{k})\right]Y_{lm}^{*}(\hat{\mathbf{k}}),\tag{183}$$

at second order.

8.2.2 Redshift-dependent relativistic galaxy counts at first order

Taking into account the dominant first-order relativistic corrections on sub-horizon scales [36, 87, 107] the redshift-dependent multipole term for galaxy counts at linear order can be written as

$$\gamma_{lm}^{L}(z) = 4\pi(-i)^{l}\int \frac{d^{3}k}{(2\pi)^{3}}\Bigg\{\left[j_{l}(k(\eta_{0}-\eta))D_{+}(z)\,\delta_{1}(\mathbf{k})\right] + \left(\frac{\mathbf{k}r_{s}}{H(z)}j_{l}''(kr_{s})\right) + (2s-5)\left[l(l+1)\int dr'\frac{r_{s}-r'}{r_{s}r'}g(r')\,\varphi_{m}j_{l}(kr_{s})\right]\Bigg\}Y_{lm}^{*}(\hat{\mathbf{k}}). \tag{184}$$

8.3 Redshift-dependent bispectrum terms

As the exact derivation of a fully relativistic expression for galaxy count terms at second order is still underway, in this section we write down the expressions for those mixed bispectrum terms which only include galaxy counts at linear order. For additional information on the derivation of relativistic galaxy counts at second order, their angular decomposition, and the pure $\gamma_{l_am_a}(z_a)\,\gamma_{l_bm_b}(z_b)\,\gamma_{l_cm_c}(z_c)$ redshift-dependent bispectrum, see [28, 44, 45]

$\tau^{\mathbf{NL}}_{\mathbf{l_am_a}}\tau^{\mathbf{L}}_{\mathbf{l_bm_b}}\gamma^{\mathbf{L}}_{\mathbf{l_cm_c}}(\mathbf{z_c})$ term

$$\frac{1}{8\pi^{6}}(-i)^{l_a+l_b+l_c}\int\left[K_0(\mathbf{k_a})\,\Delta_{l_a}^{0(2)}(k_a)+K_1(\mathbf{k_a})\,\Delta_{l_a}^{1(2)}(k_a)+K_2(\mathbf{k_a})\,\Delta_{l_a}^{2(2)}(k_a)\right]\times \left[\frac{j_{l_b}(k_b(\eta_0-\eta))}{3}\varphi_m(k_b)\right]\Bigg\{\left[j_{l_c}(k_c(\eta_0-\eta))D_{+}(z)\,\delta_1(\mathbf{k}_c)\right]+\left(\frac{k_c r(z)}{H(z)}j_{l_c}''(k_c r)\right)+ (2s-5)\left[l_c(l_c+1)\int dr'\frac{r_s-r'}{r_sr'}g(r')\,\varphi_m j_{l_c}(kr_s)\right]\Bigg\}Y_{l_am_a}^{*}(\hat{\mathbf{k}}_a)Y_{l_bm_b}^{*}(\hat{\mathbf{k}}_b)Y_{l_cm_c}^{*}(\hat{\mathbf{k}}_c)d^3k_ad^3k_bd^3k_c+ + \frac{1}{64\pi^{8}}\sum_{L_1M_1}\sum_{L_2M_2}(-i)^{l_b+l_c+L_1+L_2}\mathcal{G}^{m_aM_1M_2}_{l_aL_1L_2}\int\left[\frac{j_{l_b}(k_b(\eta_0-\eta))}{3}\varphi_m(\mathbf{k}_b)\right]\left[\varphi_*(\mathbf{k}_1)\varphi_*(\mathbf{k}_2)\Delta_{L_1L_2}(k_1,k_2)\right]\times \Bigg\{\left[j_{l_c}(k_c(\eta_0-\eta))D_{+}(z)\,\delta_1(\mathbf{k}_c)\right]+\left(\frac{\mathbf{k}_c r_s}{H(z)}j_{l_c}''(k_c r)\right)+ (2s-5)\left[l_c(l_c+1)\int dr'\frac{r_s-r'}{r_sr'}g(r')\,\varphi_m j_{l_c}(k_cr)\right]\Bigg\}\times Y_{L_1M_1}(\hat{\mathbf{k}}_1)Y_{L_2M_2}(\hat{\mathbf{k}}_2)Y_{l_bm_b}^{*}(\hat{\mathbf{k}}_b)Y_{l_cm_c}^{*}(\hat{\mathbf{k}}_c)d^3k_1d^3k_2d^3k_bd^3k_c. \tag{185}$$

$\tau^{\mathbf{NL}}_{\mathbf{l_a m_a}} \gamma^{\mathbf{L}}_{\mathbf{l_b m_b}}\left(\mathbf{z_b}\right) \gamma^{\mathbf{L}}_{\mathbf{l_c m_c}}\left(\mathbf{z_c}\right)$ **term**

$$\frac{1}{8\pi^6}(-i)^{l_a+l_b+l_c}\int\left[K_0\left(\mathbf{k}_a\right)\Delta^{0(2)}_{l_a}(k_a)+K_1\left(\mathbf{k}_a\right)\Delta^{1(2)}_{l_a}(k_a)+K_2\left(\mathbf{k}_a\right)\Delta^{2(2)}_{l_a}(k_a)\right]\times$$

$$\Bigg\{[j_{l_b}(k_b(\eta_0-\eta))D_+\left(z\right)\delta_1(\mathbf{k}_b)]+\left(\frac{\mathbf{k}_b r_s}{H(z)}j''_{l_b}\left(k_b r\right)\right)+$$

$$(2s-5)\left[l_b\left(l_b+1\right)\int dr'\frac{r_s-r'}{r_s r'}g\left(r'\right)\varphi_m j_{l_b}\left(k_b r\right)\right]\Bigg\}\times$$

$$\Bigg\{[j_{l_c}(k_c(\eta_0-\eta))D_+\left(z\right)\delta_1(\mathbf{k}_c)]+\left(\frac{\mathbf{k}_c r_s}{H(z)}j''_{l_c}\left(k_c r_s\right)\right)+$$

$$(2s-5)\left[l_c\left(l_c+1\right)\int dr'\frac{r_s-r'}{r_s r'}g\left(r'\right)\varphi_m j_{l_c}\left(k_c r_s\right)\right]\Bigg\}\times$$

$$Y^*_{l_a m_a}(\hat{\mathbf{k}}_a)Y^*_{l_b m_b}(\hat{\mathbf{k}}_b)Y^*_{l_c m_c}(\hat{\mathbf{k}}_c)d^3k_a d^3k_b d^3k_c+$$

$$+\frac{1}{64\pi^8}\sum_{L_1 M_1}\sum_{L_2 M_2}(-i)^{l_b+l_c+L_1+L_2}\mathcal{G}^{m_a M_1 M_2}_{l_a L_1 L_2}\int[\varphi_*(\mathbf{k}_1)\varphi_*(\mathbf{k}_2)\Delta_{L_1 L_2}(k_1,k_2)]\times$$

$$\Bigg\{[j_{l_b}(k_b(\eta_0-\eta))D_+\left(z\right)\delta_1(\mathbf{k}_b)]+\left(\frac{\mathbf{k}_b r_s}{H(z)}j''_{l_b}\left(k_b r_s\right)\right)+$$

$$(2s-5)\left[l_b\left(l_b+1\right)\int dr'\frac{r_s-r'}{r_s r'}g\left(r'\right)\varphi_m j_{l_b}\left(k_b r_s\right)\right]\Bigg\}\times$$

$$\Bigg\{[j_{l_c}(k_c(\eta_0-\eta))D_+\left(z\right)\delta_1(\mathbf{k}_c)]+\left(\frac{k_c r_s}{H(z)}j''_{l_c}\left(k_c r\right)\right)+$$

$$(2s-5)\left[l_c\left(l_c+1\right)\int dr'\frac{r_s-r'}{r_s r'}g\left(r'\right)\varphi_m j_{l_c}\left(k_c r_s\right)\right]\Bigg\}\times$$

$$Y_{L_1 M_1}(\hat{\mathbf{k}}_1)Y_{L_2 M_2}(\hat{\mathbf{k}}_2)Y^*_{l_b m_b}(\hat{\mathbf{k}}_b)Y^*_{l_c m_c}(\hat{\mathbf{k}}_c)d^3k_1 d^3k_2 d^3k_b d^3k_c. \tag{186}$$

8.4 ISW-Projected galaxy counts bispectra

In this section we write down the terms for the bispectrum of the integrated Sachs-Wolfe effect and cumulative galaxy counts. As illustrated in Section 7, under certain assumptions galaxy counts can be treated in the Newtonian approximation, allowing us to write down all terms of both $\langle\tau\tau\gamma\rangle$ and $\langle\tau\gamma\gamma\rangle$ mixed bispectra on the largest scales. We must stress, however that this expression is not suitable for studies which specifically aim to measure general relativistic (or modified gravity) effects through their effect on galaxy distribution, as the relevant information is lost.

$\tau^{\mathbf{NL}}_{\mathbf{l_a m_a}}\tau^{\mathbf{L}}_{\mathbf{l_b m_b}}\gamma^{\mathbf{L}}_{\mathbf{l_c m_c}}$ term

$$\begin{aligned}
&\frac{1}{8\pi^6}(-i)^{l_a+l_b+l_c}\int\left[\frac{j_{l_b}(k_b(\eta_0-\eta))}{3}\varphi_m(k_b)\right]\times\\
&\left[K_0\left(\mathbf{k}_a\right)\Delta^{0(2)}_{l_a}(k_a)+K_1\left(\mathbf{k}_a\right)\Delta^{1(2)}_{l_a}(k_a)+K_2\left(\mathbf{k}_a\right)\Delta^{2(2)}_{l_a}(k_a)\right]\times\\
&\left[j_{l_c}(k_c(\eta_0-\eta))\int_0^{\eta_H}n(z)\frac{dz}{d\eta}D_+\left(a\right)\delta_1(k_c)\right]Y^*_{l_a m_a}(\hat{\mathbf{k}}_a)Y^*_{l_b m_b}(\hat{\mathbf{k}}_b)Y^*_{l_c m_c}(\hat{\mathbf{k}}_c)d^3k_a d^3k_b d^3k_c+\\
&+\frac{1}{64\pi^8}\sum_{L_1M_1}\sum_{L_2M_2}(-i)^{l_b+l_c+L_1+L_2}\mathcal{G}^{m_a M_1 M_2}_{l_a L_1 L_2}\int\left[\frac{j_{l_b}(k_b(\eta_0-\eta))}{3}\varphi_m(\mathbf{k}_b)\right]\left[\varphi_*(\mathbf{k}_1)\varphi_*(\mathbf{k}_2)\Delta_{L_1L_2}(k_1,k_2)\right]\times\\
&\left[j_{l_c}(k_c(\eta_0-\eta))\int_0^{\eta_H}n(z)\frac{dz}{d\eta}D_+\left(a\right)\delta_1(\mathbf{k}_c)\right]Y_{L_1M_1}(\hat{\mathbf{k}}_1)Y_{L_2M_2}(\hat{\mathbf{k}}_2)Y^*_{l_b m_b}(\hat{\mathbf{k}}_b)Y^*_{l_c m_c}(\hat{\mathbf{k}}_c)d^3k_1 d^3k_2 d^3k_b d^3k_c.
\end{aligned} \tag{187}$$

$\tau^{\mathbf{NL}}_{\mathbf{l_a m_a}}\gamma^{\mathbf{L}}_{\mathbf{l_b m_b}}\gamma^{\mathbf{L}}_{\mathbf{l_c m_c}}$ term

$$\begin{aligned}
&\frac{1}{8\pi^6}(-i)^{l_a+l_b+l_c}\int\left[K_0\left(\mathbf{k}_a\right)\Delta^{0(2)}_{l_a}(k_a)+K_1\left(\mathbf{k}_a\right)\Delta^{1(2)}_{l_a}(k_a)+K_2\left(\mathbf{k}_a\right)\Delta^{2(2)}_{l_a}(k_a)\right]\times\\
&\left[j_{l_b}(k_b(\eta_0-\eta))\int_0^{\eta_H}n(z)\frac{dz}{d\eta}D_+\left(\eta\right)\delta_1(\mathbf{k}_b)\right]\times\\
&\left[j_{l_c}(k_c(\eta_0-\eta))\int_0^{\eta_H}n(z)\frac{dz}{d\eta}D\left(\eta\right)\delta_1(\mathbf{k}_c)\right]Y^*_{l_a m_a}(\hat{\mathbf{k}})Y^*_{l_b m_b}(\hat{\mathbf{k}}_b)Y^*_{l_c m_c}(\hat{\mathbf{k}}_c)d^3k_a d^3k_b d^3k_c+\\
&+\frac{1}{64\pi^8}\sum_{L_1M_1}\sum_{L_2M_2}(-i)^{l_b+l_c+L_1+L_2}\mathcal{G}^{m_a M_1 M_2}_{l_a L_1 L_2}\int\left[\varphi_*(\mathbf{k}_1)\varphi_*(\mathbf{k}_2)\Delta_{L_1L_2}(k_1,k_2)\right]\times\\
&\left[j_{l_b}(k_b(\eta_0-\eta))\int_0^{\eta_H}n(z)\frac{dz}{d\eta}D\left(\eta\right)\delta_1(\mathbf{k}_b)\right]\left[j_{l_c}(k_c(\eta_0-\eta))\int_0^{\eta_H}n(z)\frac{dz}{d\eta}D_+\left(\eta\right)\delta_1(\mathbf{k}_c)\right]\times\\
&Y_{L_1M_1}(\hat{\mathbf{k}}_1)Y_{L_2M_2}(\hat{\mathbf{k}}_2)Y^*_{l_b m_b}(\hat{\mathbf{k}}_b)Y^*_{l_c m_c}(\hat{\mathbf{k}}_c)d^3k_1 d^3k_2 d^3k_b d^3k_c.
\end{aligned} \tag{188}$$

$\gamma^{\mathbf{NL}}_{\mathbf{l_a m_a}} \tau^{\mathbf{L}}_{\mathbf{l_b m_b}} \tau^{\mathbf{L}}_{\mathbf{l_c m_c}}$ **term**

$$\frac{1}{8\pi^6}(-i)^{l_a+l_b+l_c}\int\left[j_{l_a}(k_a(\eta_0-\eta))\int_0^{\eta_H} n(z)\frac{dz}{d\eta}j_{l_a}(k_a(\eta_0-\eta))D_+^2\left(\eta\right)\delta_2(\mathbf{k}_a)\right]\times$$
$$\left[\frac{j_{l_b}(k_b(\eta_0-\eta))}{3}\varphi_m(\mathbf{k}_b)\right]\left[\frac{j_{l_c}(k_c(\eta_0-\eta))}{3}\varphi_m(\mathbf{k}_c)\right]Y^*_{l_a m_a}(\hat{\mathbf{k}}_a)Y^*_{l_b m_b}(\hat{\mathbf{k}}_b)Y^*_{l_c m_c}(\hat{\mathbf{k}}_c)d^3k_a d^3k_b d^3k_c. \tag{189}$$

$\gamma^{\mathbf{NL}}_{\mathbf{l_a m_a}} \gamma^{\mathbf{L}}_{\mathbf{l_b m_b}} \tau^{\mathbf{L}}_{\mathbf{l_c m_c}}$ **term**

$$\frac{1}{8\pi^6}(-i)^{l_a+l_b+l_c}\int\left[j_{l_a}(k_a(\eta_0-\eta))\int_0^{\eta_H} n(z)\frac{dz}{d\eta}j_{l_a}(k_a(\eta_0-\eta))D_+^2\left(\eta\right)\delta_2(\mathbf{k}_a)\right]\left[j_{l_b}(k_b(\eta_0-\eta))\times\right.$$
$$\left.\times\int_0^{\eta_H} n(z)\frac{dz}{d\eta}D\left(a\right)\delta_1(\mathbf{k}_b)\right]\left[\frac{j_{l_c}(k_c(\eta_0-\eta))}{3}\varphi_m(\mathbf{k}_c)\right]Y^*_{l_a m_a}(\hat{\mathbf{k}}_a)Y^*_{l_b m_b}(\hat{\mathbf{k}}_b)Y^*_{l_c m_c}(\hat{\mathbf{k}}_c)d^3k_a d^3k_b d^3k_c. \tag{190}$$

9 Summary and Conclusions

Despite the wealth of information the study of non-Gaussian CMB anisotropies (both primordial and secondary ones) could provide about non-linear cosmological processes, the information available even just from the analysis of the CMB power spectrum meant that they were not subject to intense study until recent years, when results from the *Planck* mission started to place the most stringent constraints on their amplitude up to now. No detection of primordial non-Gaussianity has been found, and if on one side these constraints represent one of the tightest tests of the single-field slow-roll paradigm, on the other side there are still two orders of magntiude to probe before reaching the level of non-Gaussianity predicted by single-field models of slow-roll inflation [11].

In this work we concentrated in particular on the possibility of detecting the non-Gaussian signature of a specific secondary anisotropy: the Integrated Sachs-Wolfe effect, which is caused by the time evolution of the gravitational potentials crossed by the CMB photons, resulting in a net redshift (or blueshift) of the signal [88]. While at first order the ISW effect depends on changes in the equation of state of the Universe (since, at first order in the cosmological perturbations, gravitational potentials remain costant for a flat, matter dominated Universe), its second order contribution, called the Rees-Sciama effect, is sensitive to non linear effects such as structure formation [86].

One of the greatest obstacles in detecting this effect is the weakness of its expected (non-Gaussian) signal when compared with other anisotropy sources and, most importantly, cosmic variance. To deal with the latter, studies of the mixed, three-point ISW-LSS cross-correlation function have been proposed, but they appear to produce a weak signal to noise-ratio for the ISW signal on small scales [61].

Motivated by the latest advancements in the field of wide-angle, high-redshift galaxy surveys, and by the notion that CMB-LSS cross correlation on large scales is almost exclusively due to the ISW effect, we suggested that a detection could possibly be achieved by the analysis of ISW-LSS cross-bispectra on ultra-large, near-horizon scales.

As relativistic effects on such scales cannot be neglected without a detailed study of their relevance, we considered the use of fully relativistic expressions for both ISW-generated anisotropies and the observed galaxy distribution. We thus rederived the published fully relativistic second order transfer function for ISW anisotropies [24] on low multipoles (i.e. large scales), finding a number of second order terms which may be relevant even for low multipoles, before considering the current status of research on fully relativistic studies on the galaxy distribution to second order in the cosmological perturbations.

As work in the latter field is still in progress (several articles on a few terms have been published, and a definite agreement on them has not yet been reached [44, 45, 108]), we adopted a twofold approach:

On one hand, we made use of the available relativistic corrections at first order in the galaxy number counts to write down those redshift-dependent bispectrum terms which only depend on galaxy overdensity perturbations to linear order.

On the other, we considered the possible use of cumulative galaxy counts projected along the line-of-sight (as used in [61, 92] in the Newtonian approximation) and noticed that relativistic corrections to these cumulative terms appear to be strongly suppressed. Under a few conditions regarding magnification and evolution bias, and *assuming* that relativistic corrections also remain suppressed at second order, we provided an expression for *all* mixed bispectrum terms by using the Newtonian expression for cumulative galaxy counts (while the ISW component is still treated in a fully relativistic way). We pointed out that, in addition to requiring the above (quite stringent) assumptions, this expression is not suitable for the study of relativistic effects (or modified gravity effects arising on the largest scales) on the galaxy overdensity distribution, as the relevant terms have been washed out by the approximation used.

To conclude, we note that there is much work to be done: a derivation of the signal resulting from the bispectrum terms, which will most probably require a numerical calculation, is needed, followed by an analysis of the impact of the relativistic corrections to both ISW and galaxy second order terms when compared with the standard Newtonian approximation.

A complete derivation of all galaxy overdensity relativistic corrections to second order and their relevance at the scales accessible by near-future surveys would represent a considerable progress: it would provide us the terms needed for the fully relativistic approach pursued in our derivation of the redshift-dependent bispectrum terms, and it would also represent a test for our Newtonian approximation for *cumulative* galaxy overdensity anisotropies.

Last, but certainly not least a calculation of the expected signal-to-noise ratio for different combinations of available and planned CMB and galaxy surveys is needed, and could be the subject of further research.

A N-point correlation functions

A.1 2-point correlation function and power spectrum

The two-point correlation function $\xi(\mathbf{r})$ of a distribution is defined in the terms of the joint probability of finding two objects in two small volumes

$$dP = \bar{n}^2 \left[1 + \xi(\mathbf{r})\right] dV_1 dV_2, \tag{191}$$

with $\bar{n}$ the average number density. We can therefore describe $\xi(\mathbf{r})$ in terms of the fractional excess of pairs of object at distance $\mathbf{r}$ between themselves with respect to the case of a completely random distribution. If the distribution under study is also isotropic, then $\xi(\mathbf{r})$ doesn't depend on direction, and therefore $\xi(\mathbf{r}) = \xi(r)$.

In the case of a field ϕ, if we define the (normalized) fluctuation field as

$$\Phi(\mathbf{x}, t) = \frac{\phi(\mathbf{x}, t) - \bar{\phi}}{\bar{\phi}}, \tag{192}$$

with $\bar{\phi}$ the mean value of the field, then we can define the correlation function as the joint ensemble average of the fluctuation value at two different positions

$$\xi(\mathbf{r}) \equiv \langle \Phi(\mathbf{x}) \Phi(\mathbf{x} + \mathbf{r}) \rangle . \tag{193}$$

If this function is homogeneous and isotropic, then using the following definition of Fourier Transform

$$\Phi(\mathbf{x}, t) = \int \frac{d^3k}{(2\pi)^3} e^{-i\mathbf{k}\cdot\mathbf{x}} \Phi(\mathbf{k}, t), \tag{194}$$

we can write

$$\varphi = \varphi_* \frac{F(\eta)}{F_*}, \tag{195}$$

where

$$\xi(r) \equiv \langle \Phi(\mathbf{x}) \Phi(\mathbf{x} + \mathbf{r}) \rangle = \int \langle \Phi(\mathbf{k}) \Phi(\mathbf{k}') \rangle e^{i\mathbf{k}\cdot\mathbf{x}} e^{i\mathbf{k}'\cdot(\mathbf{x}+\mathbf{r})} \frac{d^3k}{(2\pi)^3} \frac{d^3k'}{(2\pi)^3}. \tag{196}$$

Because the field is homogeneous, the result cannot depend on the position $\mathbf{x}$, which means the $\langle \Phi(\mathbf{k}) \Phi(\mathbf{k}') \rangle$ term must contain a delta function of $\mathbf{k}$ and $\mathbf{k}'$

$$\langle \Phi(\mathbf{k}) \Phi^*(\mathbf{k}') \rangle = (2\pi)^3 \delta_D \left(\mathbf{k} - \mathbf{k}'\right) P_\Phi(k). \tag{197}$$

The term $P_\Phi(k)$ is called power spectrum, and measures the amplitude of field fluctuations at a given scale. We can in fact combine 194 and 196 to see that the average square value of $\Phi(\mathbf{r}, t)$ in real space is

$$\left\langle \Phi^2(t, \mathbf{r}) \right\rangle = \int d^3k \frac{P_\Phi(k)}{k}. \tag{198}$$

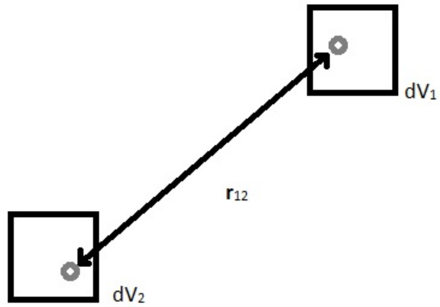

Figure 8: The two-point correlation function describes the excess probability of finding two objects in two volume elements dV_1 and dV_2 at distance r_{12} from each other, when compared to a random distribution of objects.

A.2 3-point correlation function and bispectrum

We can extend the definition of correlation function by considering the joint probability of finding N (rather than two) objects in N small volumes

$$dP = \bar{n}^N \left[1 + \xi^{(N)}\right] dV_1 dV_2 ... dV_N, \tag{199}$$

or in the case of field fluctuations

$$\xi^{(N)} = \left\langle \prod_{i=1}^{N} \left[1 + \Phi(\mathbf{r}_i)\right] \right\rangle. \tag{200}$$

In the case of the 3-point correlation function

$$\xi^{(3)} = \xi_{12} + \xi_{13} + \xi_{23} + \langle \Phi(\mathbf{r}_1)\Phi(\mathbf{r}_2)\Phi(\mathbf{r}_3)\rangle\,, \tag{201}$$

with $\xi_{ij} = \xi\,|\mathbf{r}_i - \mathbf{r}_j|$. The $\langle \Phi(\mathbf{r}_1)\Phi(\mathbf{r}_2)\Phi(\mathbf{r}_3)\rangle$ term in particular is called the *connected* three-point correlation function, and it is this term which will be the subject of this work. We will therefore omit the "connected" qualifier from now on.

The Fourier transform of the Three-point correlation function is the *bispectrum,* which is given by

$$\langle \Phi(\mathbf{k}_1)\Phi(\mathbf{k}_2)\Phi(\mathbf{k}_3)\rangle = (2\pi)^3 \delta_D \left(\mathbf{k}_1 + \mathbf{k}_2 + \mathbf{k}_3\right) B_\Phi(k_1, k_2, k_3). \tag{202}$$

An important property of both the three-point correlation function and the bispectrum is that they are identically zero for a completely Gaussian distribution, which means that their presence is a clear signal that the distribution under study is non-Gaussian.

B Wigner 3-j Symbols

B.1 Definition

The Wigner 3-j symbol

$$\begin{pmatrix} l_1 & l_2 & l_3 \\ m_1 & m_2 & m_3 \end{pmatrix}, \tag{203}$$

describes a set of three angular momenta $\mathbf{L}_1$, $\mathbf{L}_2$ and $\mathbf{L}_3$forming a triangle, with l_1, l_2, l_3 and m_1, m_2, m_3 representing their module and their z-component respectively. From the triangular condition $\mathbf{L}_1 + \mathbf{L}_2 + \mathbf{L}_3 = 0$, follows that $|l_i - l_j| \leq l_k \leq l_i + l_j$ and that $m_1 + m_2 + m_3$ must be zero. The shape of a triangle is invariant under rotations and, as such, while the coefficients m of a symbol may change under rotations, its overall configuration must not change.

B.2 Properties

The Wigner 3-j symbol is invariant for even permutations

$$\begin{pmatrix} l_1 & l_2 & l_3 \\ m_1 & m_2 & m_3 \end{pmatrix} = \begin{pmatrix} l_3 & l_1 & l_2 \\ m_3 & m_1 & m_2 \end{pmatrix}, \tag{204}$$

while it changes phase under odd permutations if $l_1 + l_2 + l_3$ is also odd

$$(-1)^{l_1+l_2+l_3} \begin{pmatrix} l_1 & l_2 & l_3 \\ m_1 & m_2 & m_3 \end{pmatrix} = \begin{pmatrix} l_1 & l_2 & l_3 \\ m_1 & m_2 & m_3 \end{pmatrix}. \tag{205}$$

For odd $l_1 + l_2 + l_3$ the symbol also changes phase under inversion of the vertical components

$$\begin{pmatrix} l_1 & l_2 & l_3 \\ m_1 & m_2 & m_3 \end{pmatrix} = (-1)^{l_1+l_2+l_3} \begin{pmatrix} l_1 & l_2 & l_3 \\ -m_1 & -m_2 & -m_3 \end{pmatrix}, \tag{206}$$

which means that the 3-j symbol

$$\begin{pmatrix} l_1 & l_2 & l_3 \\ 0 & 0 & 0 \end{pmatrix}, \tag{207}$$

is non zero only in the case when $l_1 + l_2 + l_3$is even.

The Wigner 3-j symbol also has the following orthogonality properties

$$\sum_{all\ m} \begin{pmatrix} l_1 & l_2 & l_3 \\ m_1 & m_2 & m_3 \end{pmatrix}^2 = 1. \tag{208}$$

$$\sum_{l_3 m_3} (2l_3+1) \begin{pmatrix} l_1 & l_2 & l_3 \\ m_1 & m_2 & m_3 \end{pmatrix} \begin{pmatrix} l_1 & l_2 & l_3 \\ m_1' & m_2' & m_3 \end{pmatrix} = \delta_{m_1} \delta_{m_1'} \delta_{m_2} \delta_{m_2'} \tag{209}$$

$$\sum_{m_1 m_2} \begin{pmatrix} l_1 & l_2 & l_3 \\ m_1 & m_2 & m_3 \end{pmatrix} \begin{pmatrix} l_1 & l_2 & l_3' \\ m_1 & m_2 & m_3' \end{pmatrix} = \frac{\delta_{m_1 m_1'} \delta_{m_2 m_2'}}{2l_3+1}. \tag{210}$$

B.3 The Gaunt Integral

The Gaunt integral is

$$\mathcal{G}_{l_1 l_2 l_3}^{m_1 m_2 m_3} = \int d\Omega_x Y_{l_1 m_1}(\hat{\mathbf{x}}) \, Y_{l_2 m_2}(\hat{\mathbf{x}}) \, Y_{l_3 m_3}(\hat{\mathbf{x}}) \, . \tag{211}$$

It can be written in terms of Wigner 3-j symbols as

$$\mathcal{G}_{l_1 l_2 l_3}^{m_1 m_2 m_3} = \sqrt{\frac{(2l_1+1)(2l_2+1)(2l_3+1)}{4\pi}} \begin{pmatrix} l_1 & l_2 & l_3 \\ 0 & 0 & 0 \end{pmatrix} \begin{pmatrix} l_1 & l_2 & l_3 \\ m_1 & m_2 & m_3 \end{pmatrix}. \tag{212}$$

We can easily see, by referencing the properties of the Wigner 3-j symbols seen above, that this integral is invariant under permutations, and non zero only if $m_1+m_2+m_3=0$, $l_1+l_2+l_3$ is even, and the triangle condition for l_1, l_2 and l_3 is satisfied, all of which are geometrical properties of the angular bispectrum.

References

[1] **2dFGRS** Collaboration, Colless *et al.*, *The 2dF Galaxy Redshift Survey*, Looking Deep in the Southern Sky, Proceedings of the ESO/Australia Workshop held at Sydney, Australia, 10-12 December 1997. Edited by Faffaella Morganti and Warrick J. Couch. Berlin: Springer-Verlag (1999)

[2] **6dFGS** Collaboration, Jones et al., *The 6dF Galaxy Survey: Samples, Observational Techniques and the First Data Release*, Mon. Not. R. Astr. S., **355**, 747-763 (2004), [astro-ph/0403501v1]

[3] **ACT** Collaboration, A. Fowler, *et al.*, *The Atacama Cosmology Telescope: A Measurement of the $600 < l < 8000$ Cosmic Microwave Background Power Spectrum at 148 GHz*, Astrophys. J. **722** (2), 1148–1161 (2010)

[4] **Euclid** Collaboration, R. Laureijs, J. Amiaux, S. Arduini, *et al.*, *Euclid Definition Study Report*, [arXiv:1110.3193v1]

[5] **Euclid** Collaboration, R. Scaramella, Y. Mellier, J. Amiaux, *et al.*, *Euclid space mission: a cosmological challenge for the next 15 years*, [arXiv:1501.04908v1]

[6] **LSST** Collaboration, D. Sweeney *et al.*, *Overview of the LSST Observatory System*, Am. Astr. Soc., AAS Meeting #213, id.460.01; Bulletin of the American Astronomical Society, **41**, 366 (2006)

[7] **Planck** Collaboration, R. Adam et al., *Planck 2015 results. I. Overview of products and scientific results*, Astr. and Astrophys. **594**, A1 (2016), [arXiv:1502.01582]

[8] **Planck** Collaboration, P. Ade et al., *Planck 2015 results. XIII. Cosmological parameters*, Astr. and Astrophys. **594**, A13 (2016), [arXiv:1502.01589].

[9] **Planck** Collaboration, P. Ade et al., *Planck 2015 results. XXI. The integrated Sachs-Wolfe effect*, Astr. and Astrophys. **5**94, A21 (2016), [arXiv:1502.01595]

[10] **Planck** Collaboration, P. Ade et al., *Planck 2013 results. XV. CMB power spectra and likelihood*, Astr. and Astrophys. **5**71, A15 (2014), [arXiv:1303.5075v2]

[11] **Planck** Collaboration, P. Ade et al., *Planck 2015 results. XVII. Constraints on primordial non-Gaussianity*, Astr. and Astrophys. **5**71, A15 (2014), [arXiv:1502.01592v2]

[12] **SDSS** Collaboration, F. D. Albareti *et al.*, *The Thirteenth Data Release of the Sloan Digital Sky Survey: First Spectroscopic Data from the SDSS-IV Survey Mapping Nearby Galaxies at Apache Point Observatory*, [arXiv:1608.02013]

[13] **WISE** Collaboration, E.L. Wright, P.R.M. Eisenhardt, A.K. Mainzer, *et al., The Wide-field Infrared Survey Explorer (WISE): Mission Description and Initial On-orbit Performance*, Astrophys. J., **140**, 6 (2010)

[14] **WMAP** Collaboration, D. Larson *et. al.*, *Nine Year Wilkinson Microwave Anisotropy Probe (WMAP) Observations: Cosmological Parameter Results (2012)*, [arXiv:1212.5226].

[15] D. Alonso, M. Bellini, P. G. Ferreira and M. Zumalacarregui, *The Observational Future of Cosmological Scalar-Tensor Theories*, Astroph. J. **814**, 145 (2015), [arXiv:1610.09290v1]

[16] D. Alonso, P. Bull, P. G. Ferreira *et al.*, *Ultra Large-Scale Cosmology in Next-Generation Experiments with Single Tracers*, Astroph. J. **814**, 145 (2015), [arXiv:1505.07596v3]

[17] D. Alonso, P. G. Ferreira, *Constraining ultra large-scale cosmology with multiple tracers in optical and radio surveys*, PRD, **92**, 063525 (2015), [arXiv:1507.03550v1]

[18] Afshordi, N., *Integrated Sachs-Wolfe effect in cross-correlation: The observer's manual*, PRD, **70**, 083536 (2004)

[19] N. Afshordi, Y.-S. Loh, and M. A. Strauss, *Cross-correlation of the cosmic microwave background with the 2MASS galaxy survey: Signatures of dark energy, hot gas, and point sources*, PRD 69, 083524 (2004), [astro-ph/0308260]

[20] J. M. Bardeen, P. J. Steinhardt and M. S. Turner, *Spontaneous creation of almost scale-free density perturbations in an inflationary universe*, Phys. Rev. D, **28** (1983) 679-693.

[21] N. Bartolo, E. Komatsu, S. Matarrese, A. Riotto, *Non-Gaussianity from Inflation, Theory and Observations*, Phys. Rept., **402**, 103 (2004)

[22] N. Bartolo, S. Matarrese, A. Riotto, *Enhancement of non-Gaussianity after inflation*, JHEP **0404**, 006 (2004)

[23] N. Bartolo, S. Matarrese, A. Riotto, *Gauge-Invariant Temperature Anisotropies and Primordial Non-Gaussianity*, Phys. Rev. Lett. **93**, 231301 (2004)

[24] N. Bartolo, S. Matarrese, A. Riotto, *The full Second-Order Transfer Function for Large-Scale CMB Anisotropies*, JCAP **05**, 010 (2006)

[25] C. L. Bennet *et al.*, Astrophys. J. **464**, L1 (1996)

[26] F. Bernardeau, S. Colombi, E. Gaztanaga, *et al.*, *Large scale structure of the universe and cosmological perturbation theory*, Phys.Rept. **367** (2002) 1–248, [astro-ph/0112551].

[27] D. Bertacca, A. Raccanelli, O. F. Piattella, *et al.*, *CMB-Galaxy correlation in Unified Dark Matter Scalar Field Cosmologies*, JCAP **03**, 039 (2011), [arXiv:1102.0284v2]

[28] D. Bertacca, R. Marteens, C. Clarkson, *Observed galaxy number counts on the lightcone up to second order: I. Main result*, [arXiv:1405.4403v5]

[29] M. Bilicki, T. H. Jarret, J. A. Peacock *et al., Mapping the Cosmic Web with the largest all-sky surveys*, The Zeldovich Universe: Genesis and Growth of the Cosmic Web, Proceedings of the International Astronomical Union, IAU Symposium, **308**, 143-148, [arXiv:1408.0799v1]

[30] M. Bilicki, J. A. Peacock, T. H. Jarret *et al., 2MASS Photometric redshift catalog: a comprehensive three-dimensional census of the whole sky*, The Astroph. J. Suppl., **9** (2014), [arXiv:1311.5246v2]

[31] M. Bilicki, J. A. Peacock, T. H. Jarret *et al.*, *WISE* $\times$ *SuperCOSMOS photometric redshift catalog: 20 million galaxies over 3pi steradians*, The Astrophys. J. Suppl., 2016 July, 225:5

[32] S. Boughn and R. Crittenden, *A correlation between the cosmic microwave background and large-scale structure in the Universe*, Nature 427, 45 (2004), [arXiv:astro-ph/0305001]

[33] Y. Cai, S. Cole; A. Jenkins and C. Frenk, *Towards accurate modelling of the ISW effect, the non-linear contribution*, Mon. Not. R. Astron. Soc. **396**, 772-778 (2009)

[34] S. Camera, A. Raccanelli, P. Bull, *et al.*, *Cosmology on the Largest Scales with the SKA*, [arXiv:1501.03851v2]

[35] S. M. Carroll, W. H. Press, E. L. Turner, *The cosmological constant,* Ann. Rev. Astron. & Astrophys., **30**, 499-542 (1992)

[36] A. Challinor, A. Lewis, *Linear power spectrum of observed source number counts*, PRD **84**, 043516, [arXiv:1105.5292v2]

[37] X. Chen, *Primordial Non-Gaussianities from Inflation Models*, Adv. in Astr., 638979 (2010), [arXiv:1002.1416v3]

[38] X. Chen, R. Easther and E. A. Lim, *Large non-Gaussianities in single-field inflation*, JCAP, 0706, 023 (2007)

[39] P. Coles and. F. Lucchin, Cosmology, *The origin and Evolution of Cosmic Structure*, (John Wiley & Sons, Chichester, 1995).

[40] Cooray, A., *Integrated Sachs-Wolfe effect: Large scale structure correlation*, Phys. Rev. D, **65**, 103510 (2002)

[41] B. P. Crill, P. A. R. Ade, D. R. Artusa et al., *BOOMERANG: A Balloon-borne Millimeter Wave Telescope and Total Power Receiver for Mapping Anisotropy in the Cosmic Microwave Background*, The Astrophys. J. Suppl., **148**, 527-541 (2003)

[42] R. G. Crittenden and Neil Turok, *Looking for Λ with the Rees-Sciama effect*, Phys. Rev. Lett. **76** (1996) 575, [astro-ph/9510072].

[43] M. Davis, J. Huchra, D. W. Latham, J. Tonry, *A survey of galaxy redshifts. II - The large scale space distribution*, Astrophys. J., 253, 423-445 (1982)

[44] E. Di Dio, R. Durrer, G. Marozzi, and F. Montanari, *Galaxy number counts to second order and their bispectrum*, JCAP **1412** (2014) 017, [arXiv:1407.0376]. [Erratum: JCAP1506,no.06,E01(2015)].

[45] E. Di Dio, R. Durrer, G. Marozzi, and F. Montanari, *The bispectrum of relativistic galaxy number counts*, arXiv:1510.0402v2

[46] S. Dodelson, *Modern cosmology,* Amsterdam, Netherlands: Academic Pr. (2003)

[47] M. Douspis, P. G. Castro, C. Caprini, N. Aghanim, *Optimising large galaxy surveys for ISW detection*, Astr. and Astrophys. **485**, 395-401 (2008), [arXiv: 0802.0983v1]

[48] D. J. Eisenstein, *An Analytic Expression for the Growth Function in a Flat Universe with a Cosmological Constant*, [astro-ph/9709054v2]

[49] Gaztanaga, E., Maneram, M. and Multamaki, T., *New Light on Dark Cosmos,* Mon. Not. Roy. Astron. Soc., 365, 171 (2006)

[50] T. Giannantonio, R. Scranton, R. G. Crittenden *et al.*, *Combined analysis of the integrated Sachs-Wolfe effect and cosmological implications*, PRD **77**, 123520 (2008)

[51] T. Giannantonio, R. G. Crittenden, *et al.*, *High redshift detection of the integrated Sachs-Wolfe effect*, PRD **74**, 063520 (2006), [arXiv:astro-ph/0607572]

[52] T. Giannantonio, R. Crittenden, *The effect of reionization on the cosmic microwave background-density correlation*, Mon. Not. R. Astron. Soc., **381**, 819-826 (2007)

[53] T. Giannantonio, R. G. Crittenden, *et al.*, *The significance of the integrated Sachs-Wolfe effect revisited*, Mon. Not. Astron. Soc. **426**, 2581-2599 (2012), [arXiv:1209.2125v1]

[54] T. Giannantonio, R. Scranton, R. G. Crittenden, *et al.*, *Combined analysis of the integrated Sachs-Wolfe effect and cosmological implications*, PRD **77**, 123520 (2008)

[55] T. Goto, I. Szapundi, B. R. Granett, *Cross-correlation of WISE Galaxies with the Cosmic Microwave Background*, [arXiv:1202.5306v1]

[56] B. Grinstein and M. B. Wise, , Astrophys. J. **310**, 19 (1986)

[57] A. Guth and S. Y. Pi, *Fluctuations in the new inflationary universe*, Phys. Rev. Lett. **49**, 1110 (1982)

[58] S. Ho, C. Hirata, N. Padmanabhan, *et al.*, *Correlation of CMB with large-scale structure. I. Integrated Sachs-Wolfe tomography and cosmological implications*, 2008, Phys. Rev., D **78**, 043519

[59] J. P. Huchra, L. M. Macri, K. L. Masters *et al.*, *The 2MASS redshift survey - description and data release*, the Astrophys. J. Suppl., **199**, 26 (2012)

[60] T. H. Jarret, M. E. Cluver, C. Magoulas, *et al.*, *Galaxy and Mass Assembly (GAMA): Exploring the WISE Cosmic Web in G12*, [arXiv:1607.01190v1]

[61] G. Jurgens and B. M. Schäfer, *Cross Bispectra and trispectra of the non-linear integrated Sachs-Wolfe effect and the tracer galaxy density field,* Mon. Not. Astron. Soc. **430**, 797-807 (2013)

[62] Hu, W. & Scranton, *Measuring dark energy clustering with CMB-galaxy correlations*, R., Phys. Rev. D, **70**, 123002 (2004)

[63] Kamionkowski, M., *Matter-microwave correlations in an open universe*, Phys. Rev. D, **54**, 4169-4170 (1996)

[64] E. Komatsu, N. Afshordi, N. Bartolo *et al., Non-gaussianity as a probe of the Physics of the Primordial universe and the Astrophysics of the Low Redshift universe,* Astro2010: The Astronomy and Astrophysics Decadal Survey, Science White Papers, **158**

[65] E. Komatsu & D. N. Spergel, *Acoustic signatures in the primary microwave background bispectrum,* 2001, Phys. Rev. D, **63**, 063002

[66] A. Kogut, D. Fixsen, S. Fixsen, *et al.*, *ARCADE: Absolute Radiometer for Cosmology, Astrophysics, and Diffuse Emission*, New Astronomy Reviews, **50**, 925–931 (2006)

[67] M. Liguori, E. Sefusatti, J. R. Fergusson and E.P.S. Shellard, *Primordial non-Gaussianity and Bispectrum Measurements in the Cosmic Microwave Background and Large-Scale Structure*, Adv. in Astr., 980523 (2010)

[68] A. D. Linde, *Scalar field fluctuations in the expanding universe and the new inflationary universe scenario*, Phys. Lett. B 116 335-339 (1982)

[69] A. D. Linde, V. Mukhanov, *Non-Gaussian isocurvature perturbations from inflation*, PRD, 56, 535-539 (1997)

[70] Y. Lu, F. Shi, H. J. Mo, D. Tweed, H. Wang *et al.*, *Gala***460***xy groups in the 2MASS redshift survey*, [arXiv:1607.03982v3]

[71] F. Lucchin, *Introduzione alla Cosmologia* (1998) Zanichelli

[72] F. Lucchin, S. Matarrese, Astrophys. J. , **330**, 535 (1988)

[73] C.-P. Ma, E. Bertschinger, *Cosmological Perturbation Theory in the Synchronous and Conformal Newtonian Gauges*, Astrophys. J. **455**, 7-25 (1995) [astro-ph/9506072]

[74] K. A. Malik and D. Wands, *LETTER TO THE EDITOR: Evolution of second-order cosmological perturbations*, Class. Quant. Grav. **21**, L65 (2004)

[75] S. Matarrese, F. Luchin, S. A. Bonometto, , Astrophys. J. Lett. **310**, L21 (1986)

[76] S. Mollerach, S. Matarrese, *Cosmic Microwave Background anisotropies from second-order gravitational perturbations*, [astro-ph/9702234v2]

[77] F. Montanari, R. Durrer, *Measuring the lensing potential with tomographic galaxy number counts*, [arXiv:1506.01369v3]

[78] J. R. Mould, L. Staveley-Smith, R. A. Schommer *et al.*, *The velocity field of clusters of galaxies within 100 megaparsecs. I - Southern clusters*, Astrophys. J., **383**, 467-486 (1991)

[79] J. R. Mould, R. L. Akeson, G. D. Bothun *et al.*, *The velocity field of clusters of galaxies within 100 megaparsecs. II - Northern clusters*, Astrophys. J., **409**, 14-27 (1993)

[80] J. P. Nielsen, R. Durrer, *Higher order relativistic galaxy number counts: dominating terms*, arXiv:1606.02113v2

[81] P. J. E. Peebles, *The large-scale structure of the universe* (Princeton, 1980) Princeton University Press.

[82] A. Raccanelli, F. Montanari, D. Bertacca, *et al.*, *Cosmological Measurements with General Relativistic Galaxy Correlations*, [arXiv:1505.06179v1]

[83] A. Raccanelli, O. Doré, D. J. Bacon *et al.*, *Probing primordial non-Gaussianity via iSW measurements with SKA continuum surveys*, [arXiv:1406.0010v2, 2015]

[84] C. L. Reichardt, P. A. R. Ade, J. J. Bock *et al.*, *High resolution CMB power spectrum from the complete ACBAR data set*, Astroph. J., **694**, 1200–1219 (2009)

[85] C. L. Reichardt *et al., A measurement of secondary cosmic microwave background anisotropies with two years of South Pole Telescope observations*, Astrophys. J. **755**, 70 (2012)

[86] M. J. Rees, D. W. Sciama, *Large-scale Density Inhomogeneities in the Universe*, Nature, **217**, 511-516 (1968)

[87] J. Renk, M. Zumalacarregui, F. Montanari, *Gravity at the horizon: on relativistic effects, CMS-LSS correlations and ultra-large scales in Horndeski's theory*, JCAP, **7**, 040 (2016), [arXiv:1604.03487v2]

[88] R. K. Sachs & A. M. Wolfe, *Perturbations of a Cosmological Model and Angular Variations of the Microwave Background*,, Astrophys. J., **147**, 73 (1967)

[89] V. Sahni, P. Coles, *Approximation methods for non-linear gravitational clustering*, Phys. Rep., **262**, 1-135 (1995)

[90] D. S. Salopek and J. R. Bond, PRD, 63, 063002 (2001)

[91] Santiago, B. X., Strauss, M. A., Lahav, O. et al., *The Optical Redshift Survey: Sample Selection and the Galaxy Distribution*, Astrophys. J., **446**, 457 (1995)

[92] B. M. Schäfer, *Mixed three-point correlation functions of the nonlinear integrated Sachs-Wolfe effect and their detectability,* Mon. Not. Astron. Soc. **388**, 1394-1402 (2008)

[93] R. Scranton, A. J. Connolly, R. C. Nichol, *et al.*, *Physical Evidence for Dark Energy*, [arXiv:astro-ph/0307335]

[94] P. Serra and A. Cooray, *Impact of secondary non-Gaussianities on the search for primordial non-Gaussianity with CMB maps*, PRD, **77**, 107305 (2008)

[95] S. F. Shandarin, Ya. B. Zeldovich, *The Large-Scale Structure of the Universe: Turbulence, Intermittency; Structures in a Self-Gravitating Medium*, Reviews of Modern Physics, **61** (1989)

[96] I. Smail, D. W. Hogg, R. Blandford, *et al.*, MNRAS, **277**, 1 (1995)

[97] R. E. Smith, C. Hernandez-Montegaudo and U. Seljak, *Impact of Scale Dependent Bias and Nonlinear Structure Growth on Integrated Sachs-Wolfe Effect: Angular Power Spectra*, [arXiv:0905.2408v2]

[98] G. F. Smoot, C. L. Bennet, A. Kogut *et al.*, *Structure in the COBE differential microwave radiometer first-year maps*, Astrophys. J. **396**, L1 (1992)

[99] D. N. Spergel and D. M. Goldberg, *Microwave background bispectrum. 1. Basic formalism*, Phys. Rev. **D59** (1999) 103001, [astro-ph/9811252v2].

[100] A. A. Starobinsky, *Dynamics of phase transition in the new inflationary universe scenario and generation of perturbations*, Phys. Lett. B **117** (1982) 175.

[101] M. A. Strauss, M. Davis, A. Yahil, J. Huchra, *A redshift survey of IRAS galaxies. IV - The galaxy distribution and the inferred density field*, Astrophys. J. 385, 421-444

[102] M. Tegmark *et al., Cosmological parameters from SDSS and WMAP*, Phys. Rev. D , 69, 103501 (2004)

[103] U. Seljak, *Rees-Sciama Effect in a Cold Dark Matter Universe*, Astrophys. J. **460**, 549 (1996)

[104] R. B. Tully, *Alignment of clusters and galaxies on scales up to 0.1 C*, Astrophys. J. **303,** 25–38 (1986) .

[105] M. S. Turner, M. White, *CDM models with a smooth component*, Phys. Rev. D, **56**, 4439 (1997)

[106] J. Yoo, *General Relativistic Description of the Observed Galaxy Power Spectrum: Do We Understand What We Measure?*, PRD, **82**, 083508, [arXiv:1009.3021v1]

[107] J. Yoo, A. L. Fitzpatrick, M. Zaldarriaga, *New perspective on galaxy clustering as a cosmological probe: general relativistic effects*, PRD, **80**, 083514, [arXiv:0907.0707v2]

[108] J. Yoo, M. Zaldarriaga, *Beyond the linear-order relativistic effect in galaxy clustering: Second-order gauge-invariant formalism*, [arXiv:1406.4140v1]

[109] R. van de Weygaert, R. J. Bond, *Observations and Morphology of the Cosmic Web*, Lectures at Summer School Guillermo Haro, 2005